AD_____

Award Number:
W81XWH-07-1-0059

TITLE:
Evaluation of Fibroblast Activation Protein-Alpha (FAP) as a Diagnostic Marker and Therapeutic Target in Prostate Cancer

PRINCIPAL INVESTIGATOR:
Nathaniel Brennen

CONTRACTING ORGANIZATION:
Johns Hopkins University
Baltimore, MD 21218-2686

REPORT DATE:
December 2009

TYPE OF REPORT:
Annual Summary

PREPARED FOR: U.S. Army Medical Research and Material Command
Fort Detrick, Maryland 21702-5012

DISTRIBUTION STATEMENT:

X Approved for public release; distribution unlimited

REPORT DOCUMENTATION PAGE

Form Approved
OMB No. 0704-0188

1. REPORT DATE *(DD-MM-YYYY)*	**2. REPORT TYPE**	**3. DATES COVERED** *(From - To)*
01-12-2009	Annual Summary	1 DEC 2006 - 30 NOV 2009

4. TITLE AND SUBTITLE
Evaluation of Fibroblast Activation Protein-Alpha (FAP)

as a Diagnostic Marker and Therapeutic Target in Prostate Cancer

5a. CONTRACT NUMBER

5b. GRANT NUMBER
W81XWH-07-1-0059

5c. PROGRAM ELEMENT NUMBER

6. AUTHOR(S)
W. Nathaniel Brennen

5d. PROJECT NUMBER

5e. TASK NUMBER

5f. WORK UNIT NUMBER

7. PERFORMING ORGANIZATION NAME(S) AND ADDRESS(ES)

The Johns Hopkins University
School of Medicine
Baltimore, MD 21231
E-Mail: wbrenne2@Jhmi.edu

8. PERFORMING ORGANIZATION REPORT NUMBER

9. SPONSORING / MONITORING AGENCY NAME(S) AND ADDRESS(ES)
U.S. Army Medical Research
and Material Command
Fort Detrick, Md 21702-5012

10. SPONSOR/MONITOR'S ACRONYM(S)

11. SPONSOR/MONITOR'S REPORT NUMBER(S)

12. DISTRIBUTION / AVAILABILITY STATEMENT
Approved for public release; distribution unlimited

13. SUPPLEMENTARY NOTES

14. ABSTRACT

Background: It has been well documented that the tumor is dependent upon the reactive stroma for survival and growth signals, as well as, the nutritional support necessary for the maintenance of the primary mass. Additionally, the ability of the stroma to not only contribute to, but potentially drive, the progression of cancerous cells into a highly aggressive and metastatic phenotype is a concept that has only recently begun to be appreciated. The stroma has been shown to undergo morphological alterations, recruit reactive fibroblasts, macrophages, and lymphocytes, increase secretion of growth factors, signaling molecules and proteases, induce new blood vessel formation, as well as, produce an altered extracellular matrix when associated with a transformed epithelium. Fibroblasts, in particular, have been shown to consistently undergo several changes in both morphology and expression profiles when present in the tumor microenvironment. One defining characteristic of these carcinoma-associated fibroblasts, or myofibroblasts, is the expression of fibroblast activation protein-alpha (FAP). FAP is a membrane-bound serine protease that has both dipeptidase, as well as, gelatinase and collagenase activity. FAP is not expressed in healthy adults, but has been shown to be selectively expressed on myofibroblasts in the stroma surrounding >90% of epithelial cancers examined, including 7/7 human prostate cancer specimens, with minimal to no expression in either cancerous epithelial or adjacent normal tissues. FAP has been implicated in tumor promotion through studies demonstrating increases in tumor incidence, growth, and microvessel density using in vivo models. In contrast, other studies have shown that expression of FAP decreased tumorigenicity in vivo suggesting that the physiologic response to FAP may be dependent upon the exact context of its expression.

Objective/Hypothesis: Our goal is to evaluate FAP expression patterns and enzymatic activity in both normal prostate tissue and at various stages of oncogenic transformation (i.e. PIA, PIN, Localized and Advanced Cancer) to determine tumor stage in which FAP expression may play a role. A second objective is to exploit this expression in the treatment of prostate cancer by developing therapies targeted for activation by FAP. This will be accomplished by identifying selective peptide substrates for the proteolytic activity of FAP and coupling these peptides to a highly cytotoxic agent, thapsigargin, to generate prodrugs that are only activated in prostate tumors where FAP is expressed.

Specific Aims:

1) Characterize the expression patterns of FAP in normal prostate tissue and in the disease state.
2) Identify a FAP-specific cleavable peptide sequence for the development of targeted prodrugs.
3) Synthesize prodrug and measure kinetics in vitro.
4) Determine the potential therapeutic benefit and toxicity of this prodrug in vivo.

Study Design: We will generate and characterize clones of various prostate cancer cell lines (LNCaP, C4-2, C4-2B4, and PC3) expressing FAP or an empty vector control. Primary human prostate cancer tissue specimens representing varying stages of prostate cancer, as well as, adjacent normal tissue will be stained for FAP expression and quantified. FAP-specific peptide substrates will be identified in a complementary approach using a solution-phase phage display library and a positional scanning synthetic combinatorial library. Optimal substrate sequences will be coupled to thapsigargin, a highly cytotoxic compound. Kinetics of hydrolysis, as well as, specificity and stability will be measured in vitro using the FAP-expressing clones. Lead prodrugs identified in vitro will be used to treat xenografts derived from FAP-expressing clones and mock-transfected controls to determine potential therapeutic efficacy in vivo. **Impact:** Metastatic epithelial cancers, such as those of the prostate, are composed of heterogeneous populations of cells that can have variable responses to anti-tumor agents. Currently utilized standard antiproliferative chemotherapies can produce modest improvement in survival in select cancer types, but are largely ineffective in treating malignancies of the prostate (proliferative index < 5%). Novel therapies that act in a proliferation-independent manner, therefore, are urgently needed for the treatment of advanced prostate cancer. An emerging strategy has been to target the stromal components associated with the tumor. One potential therapy is the development of prodrugs activated by proteases selectively expressed in the stromal compartment as outlined in this proposal. This approach will effectively deliver a cytotoxic molecule, such as thapsigargin, in a highly specific manner to the tumor microenvironment and will directly result in significant stromal cell death and indirectly in epithelial mortality due to a bystander effect with limited systemic toxicity.

15. SUBJECT TERMS
Prodrug, Fibroblast, Protease

16. SECURITY CLASSIFICATION OF:			**17. LIMITATION OF ABSTRACT**	**18. NUMBER OF PAGES**	**19a. NAME OF RESPONSIBLE PERSON**
a. REPORT	**b. ABSTRACT**	**c. THIS PAGE**			USAMRMC
U	U	U	UU	43	**19b. TELEPHONE NUMBER** *(include area code)*

Standard Form 298 (Rev. 8-98)
Prescribed by ANSI Std. Z39.18

Table of Contents

Page Number

Introduction

It has been well documented that the tumor is dependent upon the reactive stroma for survival and growth signals, as well as, the nutritional support necessary for the maintenance of the primary mass. Additionally, the ability of the stroma to not only contribute to, but potentially drive, the progression of cancerous cells into a highly aggressive and metastatic phenotype is a concept that has only recently begun to be appreciated. The stroma has been shown to undergo morphological alterations, recruit reactive fibroblasts, macrophages, and lymphocytes, increase secretion of growth factors, signaling molecules and proteases, induce new blood vessel formation, as well as, produce an altered extracellular matrix when associated with a transformed epithelium. Fibroblasts, in particular, have been shown to consistently undergo several changes in both morphology and expression profiles when present in the tumor microenvironment. One defining characteristic of these carcinoma-associated fibroblasts, or myofibroblasts, is the expression of fibroblast activation protein-alpha (FAP). FAP is a membrane-bound serine protease that has both dipeptidase, as well as, gelatinase and collagenase activity. FAP is not expressed in healthy adults, but has been shown to be selectively expressed on myofibroblasts in the stroma surrounding >90% of epithelial cancers examined, including 7/7 human prostate cancer specimens, with minimal to no expression in either cancerous epithelial or adjacent normal tissues. FAP has been implicated in tumor promotion through studies demonstrating increases in tumor incidence, growth, and microvessel density using in vivo models. In contrast, other studies have shown that expression of FAP decreased tumorigenicity in vivo suggesting that the physiologic response to FAP may be dependent upon the exact context of its expression. Our goal is to evaluate FAP expression patterns and enzymatic activity in both normal prostate tissue and at various stages of oncogenic transformation (i.e. PIA, PIN, Localized and Advanced Cancer) to determine tumor stage in which FAP expression may play a role. A second objective is to exploit this expression in the treatment of prostate cancer by developing therapies targeted for activation by FAP. This will be accomplished by identifying selective peptide substrates for the proteolytic activity of FAP and coupling these peptides to a highly cytotoxic agent, thapsigargin, to generate prodrugs that are only activated in prostate tumors where FAP is expressed.

Body

Hypothesis and Objective

Our hypothesis is that FAP is expressed on the surface of myofibroblasts in the stroma surrounding the majority of malignant prostatic lesions and that this expression can be taken advantage of for clinical benefit. The goal of this proposal is to investigate FAP expression patterns in normal prostate tissue and prostate cancers at various stages and to develop novel FAP-activated prodrug therapies that exploit FAP's tumor stroma restricted expression in the treatment of prostate cancer. Furthermore, due to the localized expression of FAP to the stroma associated with tumors from multiple tissues of origin, this therapy may have the potential to effectively treat a broad spectrum of epithelial malignancies.

Specific Aims 1: Characterize the expression patterns of FAP in normal and hyperplastic prostate tissue and in various stages of prostate cancer

Limited information is available on expression of FAP in prostate tissue. Initial studies characterizing FAP expression in epithelial cancers did not include prostate cancer. The only data showing FAP expression is by Tuxhorn et al. who demonstrated expression in 7/7 samples of localized prostate cancer taken from core biopsies. Our goal, therefore, is to perform more extensive analysis of FAP expression in normal prostate, BPH, and various stages of prostate cancer including premalignant proliferative inflammatory atrophy (PIA), prostatic intraepithelial neoplasia (PIN), in addition to, various stages and grades of PCa, including organ-confined, androgen-dependent adenocarcinomas and hormone-refractory metastatic bone lesions. Studies to date on human tissue have relied on the commercially available F19 mouse anti-human FAP hybdridoma which we have available in our laboratory. A second mouse anti-FAP antibody has been purchased from Bender MedSystems. Both antibodies only recognize native FAP and only work on frozen tissue and in FACS analysis. The goal of these studies will be to determine the prognostic significance of FAP expression in human prostate cancer and to begin to gain an understanding of whether FAP may play a role in the pathobiology of the disease.

We were unable to work out a satisfactory staining protocol for any of the commercially available antibodies during the project period, however, we are continuing alternative protocols to optimize staining and would like to complete these studies in the future when they become possible.

Specific Aim 2: Identify a FAP-specific cleavable peptide sequence for the development of targeted prodrugs delivering a toxin (i.e., thapsigargin).

Peptide sequences specifically cleaved by FAP's enzymatic activity will be identified through the coordinated application of two different techniques. The first approach will be to perform traditional mapping of FAP cleavage sites within collagen I, a known FAP protein substrate. Dr. Denmeade's lab recently completed this digestive approach using recombinant collagen I derived gelatin produced in E coli so that no post-translational modifications occurred (i.e. proline hydroxylation). FAP cleavage sites within this gelatin were determined using LC-MS analysis performed in collaboration with Dr. Robert Cotter's group at Johns Hopkins who specialize in mass spectrometric-based proteomic techniques. This study yielded a large number of cleavage sites within the gelatin, but given that collagen is a heterotrimeric polymer made up of repeating sequences containing the (GXY)n motif (X= Pro, Y= HydroxyPro), the cleavage sites were of a limited repertoire. To obtain more complete analysis of FAP substrate requirements we will synthesize a positional scanning synthetic combinatorial library (PSSCL) employing a 4-amino-7-carbamoylmethylcoumarin (ACC) based resin that will enable the P1-P6 subsite specificity of the putative FAP substrates to be probed in a high throughput manner. The combined integration of consensus sequences detected through each of these screens should allow the identification of highly-specific FAP cleavable peptide sequences that can be linked to a highly cytotoxic compound such as thapsigargin to generate a prodrug that is selectively activated by FAP-positive reactive stromal cells within prostate cancer sites while avoiding toxicity to normal FAP-negative host tissues.

The cleavage products generated from the Collagen I derived gelatin digestion were ranked according to their normalized ion current. This value was calculated by extracting the ion current for the parent mass of the ion from the total MS ion chromatogram and then integrating under the peak from the liquid chromatogram. This ranking was performed in an attempt to quantify the relative abundance of each fragment within the mixture and consequently a preferred cleavage motif (Figure 4 of Appendix A). The frequency of individual amino acids within the P7-P1' positions of each cleavage site were also determined to reveal a consensus peptide containing optimal residues in each position The basic pattern that emerged from this analysis was (D/E)-(R/K)-G-(E/D)-(A/G/S/T)-G-P-A or (acidic aa)-(basic aa)-G-(acidic aa)-(Small/Polar-OH aa)-G-P-A (Figure 5 of Appendix A).

As a result of these analyses we selected several peptides representing high, intermediate, and low extracted ion currents from the gelatin digestion products, as well as, variations of the consensus peptide for further study. Fluorescence-quenched substrates based on the selected sequences were synthesized in order to ascertain Michaelis-Menten kinetic parameters (i.e. K_m, V_{max}, k_{cat}) of FAP hydrolysis. Substrates were ranked according to their calculated k_{cat}/K_m ratios (Table 2 & 3 of Appendix A). In general, those substrates with the highest extracted ion currents were cleaved the most efficiently by FAP indicating that this normalization method is of benefit in identifying preferred cleavage motifs from digestion products. The critical importance of an amino acid in the P1' position was demonstrated based on the near abrogation of hydrolysis in substrates lacking a residue in this position. There was minimal improvement observed in substrates with additional amino acids on the P' side beyond the P1' position. See appended publication, 'Fibroblast Activation Protein (FAP) Peptide Substrates Identified from Human Collagen I-derived Gelatin Cleavage Sites' (Aggarwal, 2007) for additional information regarding methods and a more detailed discussion of the results found related to this aim. Synthesis of several fluorescence-quenched substrates containing hydroxyproline in the Y positon of the collagen (GXY)n motif has been performed in order to determine the potential role of this post-translational modification in relation to FAP's efficiency of hydrolysis.

Synthesis of the 4-amino-7-carbamoylmethylcoumarin (ACC) fluorophore for use in the positional scanning synthetic combinatorial library (PSSCL) was completed successfully after enlisting the aid of Dave Meyers, director of the Pharmacology Synthesis Core on campus. Unfortunately, were unable to demonstrate cleavage of peptides generated with this fluorophore by FAP for reasons that are not entirely clear, but likely stem from steric hindrance associated with the bulky fluorophore in the P1' position.

Specific Aim 3: Synthesize prodrug and measure kinetics in vitro using both human prostate cancer cell lines and cell-free assays.

Prodrugs have been generated from the sequences identified in Specific Aim 2 by linking them via a peptide bond to amino acid containing 12ADT analogs. Specifically, sequences No.1 ASGPAGPA, No.3 DRGETGPA, No.13 DSGETGPA, and No.14 ERGETGPS from Table 2 of the appended publication, 'Fibroblast Activation Protein (FAP) Peptide Substrates Identified from Human Collagen I-derived Gelatin Cleavage Sites' (Aggarwal, 2007) were selected based upon their *in vitro* kinetic parameters, as well as, solubility concerns. All four of these prodrugs were found to be proteolytically activated by FAP with parameters comparable to those observed for hydrolysis of the fluorescence-quenched substrates. In an *in vitro* assay, release of the active form of the prodrugs (A- or S- 12ADT) was monitored and confirmed by LC/MS analysis (Figure 1). Two non-FAP cleavable controls were generated based upon our lead sequence, one is a scrambled analog (PETGRSG-E12ADT) and one has the P1-Pro residue of the cleavage site converted to a d-isomer (ERGETGp-S12ADT). Neither of these control analogs are hydrolyzed by FAP to the active form under the tested conditions.

Thapsigargin and its analogs function by inhibition of the SERCA pump, which leads to a critical elevation in cytoplasmic [Ca^{2+}] that triggers apoptosis. Using a cell permeable calcium dye we demonstrated that these compounds in their full-length, or non-cleaved, prodrug form are unable to induce a rise in cytosolic [Ca^{2+}], and

thus are inactive (Figure 2). In contrast, the active forms of the drugs generate a rapid rise in [Ca^{2+}] levels within minutes of administration to a viable cell suspension.

A soluble, extracellular form of FAP has previously been identified in bovine serum (Collins, 2004) and we report here that FAP activity is present in the fetal (FBS) version as well. We were able to take advantage of this presence to selectively activate our prodrugs in tissue culture media. We demonstrated that all three FAP-activated prodrugs were hydrolyzed in media supplemented with 10% FBS reaching low [nM] of the active drug, but not in its absence (Figure 3). Next, these prodrugs were added to the media and incubated with the MCF-7 breast cancer cell line to determine their potency in vitro. MCF-7 cell growth was inhibited by 50% at a mean concentration of ~3.5nM by the FAP-activated prodrugs. In contrast, both the scrambled and d-isomer analog (non-FAP cleavable) controls were at least 300-fold less potent with IC_{50}'s greater than 1μM (Table 1).

Specific Aim 4: Determine the potential therapeutic benefit and toxicity of prodrugs in vivo using human prostate cancer xenografts in immunocompromised murine hosts.

FAP expression has been more extensively studied in the context of breast cancer. Consequently, we decided to initially test the efficacy of the FAP-activated prodrugs in human xenograft models of breast cancer using the MCF-7 cell line prior to moving into the less well characterized models of prostate cancer. First, we determined that murine fibroblasts that have infiltrated the tumor compartment of MCF-7 xenografts express the mouse homolog of FAP (Figure 4), which shares 89% sequence homology including the catalytic triad, and take on a reactive phenotype similar to that seen in human CAFs. McKee, et al., have demonstrated measurable FAP activity in human plasma as part of the fibrinolysis pathway (Lee, 2006). This observation led us to investigate whether the same activity was present in mouse plasma. Based upon the hydrolysis of a FAP-selective fluorescence quenched peptide substrate described previously (Aggarwal, 2007) we demonstrate that FAP-like enzymatic activity is present in mouse plasma as well (Figure 5). As further evidence we show that this hydrolysis is abrogated by a FAP-selective inhibitor, Acetylated-Gly-boroPro (AcGbP) (Edosada, 2006). When comparing the amount of FAP activity present in the plasma/serum from various species it is evident that there is significantly greater activity in the mouse, up to 10-fold compared to human, based upon the rate of substrate hydrolysis (Figure 5). While this activity clearly has implications for the stability of the FAP-activated prodrugs in mouse plasma we decided to pursue the efficacy studies using this model despite these challenges. The rationale being, that if we could achieve a therapeutic benefit with minimal toxicity to the host in spite of this high level of activity it would presumably translate into an even greater therapeutic window in models that more accurately represent the level of FAP present in human plasma.

In order to move into in vivo efficacy experiments utilizing MCF-7 xenografts in female nude mice we first had to determine a maximum tolerated dose (MTD). We determined that three consecutive daily IV injections of 100nmoles of each of the prodrugs exhibited no significant toxicity in the hosts during an observation period greater than 1 month (Table 2). Notably, we reached an LD_{100} at 10nmoles of the active form of the drug (A12ADT) and could only administer a dosing solution that was 1% of that given for the prodrugs without observing mortality. This translates into a 30-fold increase in the therapeutic window of the thapsigargin analog when administered in the prodrug form. The most rapid onset of morbidity at the 1000nmole dosing level was observed with the ERGETGP-S12ADT prodrug and for this reason we chose to eliminate it from the initial efficacy studies.

Based upon this toxicity/survival study we chose to move forward with a dosing regimen consisting of three consecutive daily injections of a 100nmole IV dose. We observed a significant inhibition in tumor growth compared to untreated controls that persisted for greater than 1 month following two courses of the stated treatment regimen with the FAP-activated prodrug, but not with the scrambled and d-isomer analogs (Figure 6A). No significant toxicity, defined as >10% loss in body weight, was observed in the treatment groups over the treatment period compared to the untreated controls (Figure 6B). The scrambled and d-isomer analog arms of the study were terminated early because they demonstrated no significant difference in tumor growth

compared to the control group and were used for preliminary immunohistochemical analyses. Efficacy of the FAP-activated prodrugs was evaluated in four independent experiments and demonstrated a consistent anti-tumor effect (Figure 6C) with minimal weight loss associated with treatment (Figure 6D). The plasma half-life ($t_{1/2}$) of the ASGPAGP-A12ADT full-length prodrug was determined to be ~5.3hrs in a nude mouse with no accumulation seen at 24hrs following the second and third doses (Figure 6E). Additionally, we observed minimal activation (<0.1%) of the prodrugs to the active form in the plasma during this period.

Immunohistochemical analysis of MCF-7 xenografts confirmed stromal-selective cell death in tumors treated with a FAP-activated prodrug (Figure 7). Tumors were harvested 24hrs following the third dose of a FAP-activated and compared to untreated controls. As predicted based upon the therapeutic strategy employed there is a strong correlation between regions of FAP expression and TUNEL-positive nuclei (Figure 7A). We also observe occasional patches of epithelial carcinoma cells that are TUNEL-positive in areas immediately adjacent to the FAP-positive stroma suggestive of a bystander effect. Quantitatively, there is nearly 90% more TUNEL-positive nuclei in the tumors treated with a FAP-activated prodrug compared to the untreated controls (Figure 7B).

Since FAP is also expressed on intra-tumoral pericytes (Figure 7C, right) (Ramirez-Montagut, 2004) found in association with vascular endothelial cells in tumors (Figure 7C, left) we wanted to determine whether our prodrugs also had an effect on this cell population. We observe CD31-positive endothelial cells with TUNEL-positive nuclei in tumors treated with a FAP-activated prodrug (Figure 7D) indicating the efficacy against this tumor may be derived from an anti-angiogenic effect in addition to targeting the CAF population. Despite this induction of endothelial cell death there was no difference in the overall amount of CD31 expression observed in tumors between treated and untreated groups (data not shown). This lack of a difference in total vessel area could be a result of collecting the tissues 24hrs after the first cycle of therapy, which may be at a point before this loss in expression would be observed.

While we do see a strong correlation between FAP expression and TUNEL-positive nuclei there also does not appear to be a significant reduction in overall FAP levels within the tumor (Figure 7, A and E). Once again, one explanation for this observation may be the early collection time for the tissues. Another possibility is that the remaining fibroblasts may begin to proliferate once the initial pool of CAFs begins to undergo apoptosis. Alternatively, signals may be released that induce mesenchymal stem cells (MSCs) to invade and differentiate in order to re-populate this pool of FAP-expressing cells. This second possibility was examined by analyzing the number of cells that expressed Ki-67 using a monoclonal antibody specific to the mouse homolog. Interestingly, we find that there is a 5-fold increase in stromal cell proliferation following treatment with the FAP-activated prodrug compared to the untreated controls (Figure 7, E and F), which raises the possibility of adjuvant therapy with an anti-proliferative drug for a more durable response. We cannot rule out an additional contribution by MSCs or a difference in FAP levels at a later time point from these results.

We have several future studies planned to investigate the further potential of FAP as a prospective therapeutic target. These include direct comparisons of the biodistribution profiles of a FAP-activated prodrug (ERGETGP-S12ADT) and its non-FAP cleavable analog (ERGETGp-S12ADT) to determine the relative specificity of the prodrugs in the mouse host. We are currently investigating the therapeutic effect of these prodrugs in LNCaP xenograft models of prostate cancer and this data should be available in the near future. Studies such as this in additional tumor models will evaluate the potential use of FAP-activated prodrugs as pan-tumor therapies. A proof-of-principle experiment employing local delivery of a FAP-activated protoxin has demonstrated anti-tumor efficacy against both breast and prostate cancer xenografts (Lebeau, 2009; see Appendix B). Additionally, we plan to evaluate these prodrugs in combination trials with traditional proliferation-dependent chemotherapeutic compounds.

Key Research Accomplishments

- Digestion and analysis of human Collagen I-derived gelatin using a tandem LC-MS/MS approach
- Ranking of digestion products according to extracted ion
- Identification of preferred cleavage motifs within the human Collagen I-derived gelatin digestion products
- Identification of a consensus peptide containing optimal residues in each position, P7-P1'. The basic pattern that emerged from this analysis was (D/E)-(R/K)-G-(E/D)-(A/G/S/T)-G-P-A or (acidic aa)-(basic aa)-G-(acidic aa)-(Small/Polar-OH aa)-G-P-A.
- Synthesis of several fluorescence-quenched peptide substrates based on sequences identified and selected from the digestion products
- Determination of the Michaelis-Menten kinetic parameters (i.e. K_m, V_{max}, k_{cat}) for FAP hydrolysis of each of these substrates and ranking according to their k_{cat}/K_m ratios.
- Validation of normalization & ranking according to the extracted ion current demonstrating a novel method for identifying preferred cleavage sites
- Requirement for residue occupying P1' position of FAP substrate and minimal improvement with addition of >1aa on the P' side.
- Four FAP-activated prodrugs have been generated from the sequences identified in Specific Aim 3 by linking them via a peptide bond to amino acid containing 12ADT analogs.
- All four putative FAP-activated prodrugs, but not their analog controls, were confirmed to be proteolytically activated by FAP in an *in vitro*.
- Prodrugs were found to have a differential ability to elevated intracellular calcium depending on whether they were in the active or pro- form.
- The prodrugs were confirmed to undergo hydrolysis in tissue culture media supplemented with 10% FBS but not in its absence.
- Confirmed that mice injected sub-cutaneously with tumorigenic human epithelial cells form tumors composed of the implanted cell line, as well as, murine stromal cells that have infiltrated the xenograft. A subset of these stromal cells were found to express the mouse homolog of FAP (mFAP).
- A maximum tolerated dose (MTD) of 6-7mg/kg (0.1mmoles) IV for each of the prodrugs was determined for immunocompromised mice.
- FAP-activated prodrugs demonstrated a reproducible anti-tumor effect against MCF-7 breast cancer xenografts while the non-FAP cleavable analogs did not.
- No significant weight loss or toxicity was associated with the treatment regimens used.
- Half-life of the ASGPAGP-A12ADT FAP-activated prodrug was determined to be ~5.3hrs in mouse plasma with no accumulation of the prodrug seen at 24hrs following the second and third doses.
- Activation of the prodrug in mouse plasma in vivo represents less than <0.1% of the total amount given and is cleared rapidly.
- ~2-fold greater apoptotic nuclei (TUNEL-positive) were observed in tumors treated with a FAP-activated prodrug compared to untreated controls.
- Tumors treated with a FAP-activated prodrug demonstrated a stromal-selective pattern of cell death with some evidence of a bystander effect in cells (epithelial and endothelial) adjacent to FAP expression.
- ~5-fold greater proliferation was observed in the stromal compartment of tumors treated with a FAP-activated prodrug compared to untreated controls.
- Intratumoral delivery of a FAP-activated protoxin (Promelittin) inhibits growth of both LNCaP (prostate) and MCF-7 (breast) xenografts.

Reportable Outcomes

- **Brennen WN**, Rosen DM, Denmeade SR. Fibroblast Activation Protein (FAP): Targeting the Reactive Stroma as a Novel Prodrug Therapy. *Manuscript in Preparation*
- Lebeau A, **Brennen WN**, Aggarwal S, Denmeade SR. Targeting the Cancer Stroma with a Fibroblast Activation Protein-Activated Promelittin Protoxin. *Mol Cancer Ther*, 2009, May; 8(5): 1378-1386.
- Aggarwal S, **Brennen WN**, Kole TP, Schneider E, Topaloglu O, Yates M, Cotter RJ, Denmeade SR. Fibroblast Activation Protein (FAP) Peptide Substrates Identified from Human Collagen I-derived Gelatin Cleavage Sites. *Biochemistry*, 2008 Jan 22; 47(3): 1076-86.
- **Brennen WN**, Aggarwal S, Kole T, Rosen DM, Denmeade SR. Fibroblast Activation Protein (FAP): Targeting the Reactive Stroma as a Novel Prodrug Therapy. Multi-Institutional Prostate Cancer SPORE 2008.
    - 1-Slide Oral Platform Presentation
- **Brennen WN**, Aggarwal S, Kole, TP, Topaloglu O, Schneider E, Becker R, Denmeade SR. Fibroblast Activation Protein (FAP): Targeting the Reactive Stroma as a Novel Prodrug Therapy. May 2007. Fellow Research Day, Sidney Kimmel Comprehensive Cancer Center at Johns Hopkins; Baltimore, MD. – Honorable Mention
- **Brennen WN**, Aggarwal S, Kole TP, Yates M, Rosen M, Denmeade SR. Fibroblast Activation Protein (FAP): Targeting the Reactive Stroma as a Novel Prodrug Therapy. Oct 2007. 5th General Meeting of the International Proteolysis Society; University of Patras, Greece.
- **Brennen WN**, Aggarwal S, Kole T, Topaloglu O, Schneider E, Becker R, Denmeade SR. Fibroblast Activation Protein (FAP): Targeting the Reactive Stroma as a Novel Prodrug Therapy. Prostate Cancer (Special AACR meeting). 2006.

Conclusion

The goals of this proposal were (1) to characterize the expression of FAP, a serine protease that is selectively expressed by reactive tumor stromal fibroblasts, in human prostate cancers and (2) to identify selective substrates for the unique proteolytic activity of FAP that can be incorporated into peptide-TG prodrugs that are selectively activated only within FAP-producing prostate cancer sites. Due to technical difficulties we were unable to complete the first aim of the proposal at this time, but hope to revisit this subject once these limitations are overcome. We have identified consensus motifs from FAP digested human collagen I-derived gelatin and ranked them according to their Michaelis-Menten kinetic parameters based on the hydrolysis of their respective fluorescence-quenched peptide substrates. Several promising candidate sequences have been identified and were used to generate potential FAP-selective prodrugs. These candidate prodrugs have been confirmed to be activated by FAP's enzymatic activity, as well as, demonstrated a reproducible anti-tumor effect in multiple efficacy studies using the MCF-7 xenograft model of breast cancer. Tumors treated with a FAP-activated prodrug demonstrated a stromal-selective pattern of cell death compared to untreated control tumors. There is also evidence of a bystander effect in cells (epithelial and endothelial) adjacent to areas of FAP expression. These studies clearly validate FAP as a promising target for the activation of a systemically delivered cytotoxic prodrug within the breast cancer microenvironment. Preliminary proof-of-principle experiments employing local delivery of a FAP-activated protoxin have demonstrated inhibition of tumor growth in prostate cancer xenografts. Ongoing experiments will evaluate the efficacy of these prodrugs delivered systemically against xenograft models of prostate cancer. Further studies are needed to determine if a FAP-activated prodrug strategy would also be of therapeutic benefit in a variety of other tumor types characterized by the presence of FAP-positive cells in the reactive stroma. It will be interesting to see if we can create a greater therapeutic window in models, such as the rat, that more accurately represent the level of FAP activity present in human plasma or by combination therapy with traditional proliferation-dependent chemotherapeutic drugs. This study also provides further evidence that targeting the stroma, independent of the cancer cells themselves, is viable strategy for cancer management.

References

Collins PJ, McMahon G, O'Brien P, O'Connor B. Purification, identification and characterisation of seprase from bovine serum. Int J Biochem Cell Biol 2004;36(11):2320-33.

Edosada CY, et al. Selective inhibition of fibroblast activation protein protease based on dipeptide substrate specificity. JBC. Mar. 17; 281(11):7437-44. 2006.

Lee KN, et al. Antiplasmin-cleaving enzyme is a soluble form of fibroblast activation protein. Blood. Feb. 15; 107(4): 1397-404. 2006.

Ramirez-Montagut T, Blachere NE, Sviderskaya EV, Bennett DC, Rettig WJ, Garin-Chesa P, et al. FAPalpha, a surface peptidase expressed during wound healing, is a tumor suppressor. Oncogene 2004;23(32):5435-46.

See Attached Appendix

Supporting Data

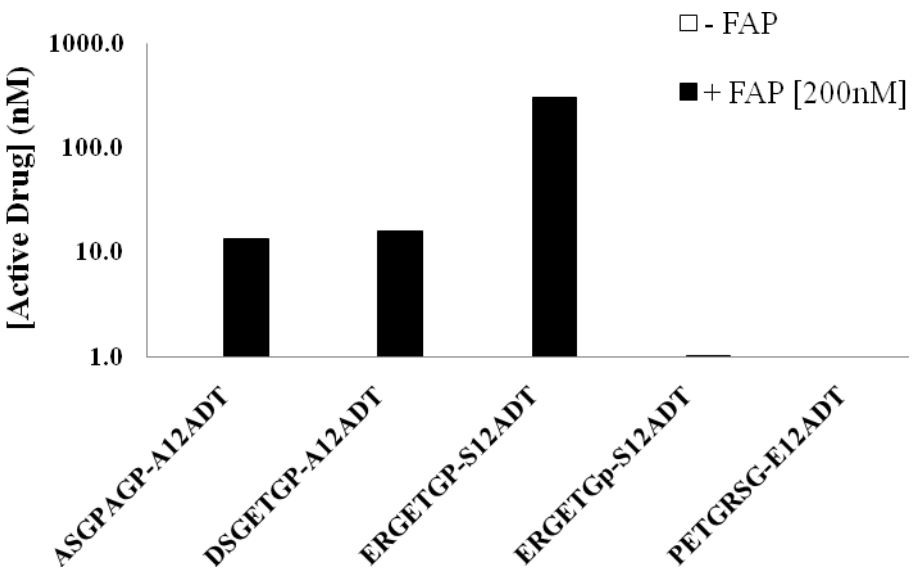

Figure 1: Release of Active Drug (A/S12ADT) from FAP Prodrugs by FAP's enzymatic activity
Prodrugs ([100µM]) were incubated with[200nM] FAP at 37°C for 24h. Aliquots were taken at the indicated time points and concentration of free drug (A/S12ADT) was determined by LC/MS. D-isomer proline represented by 'p'.

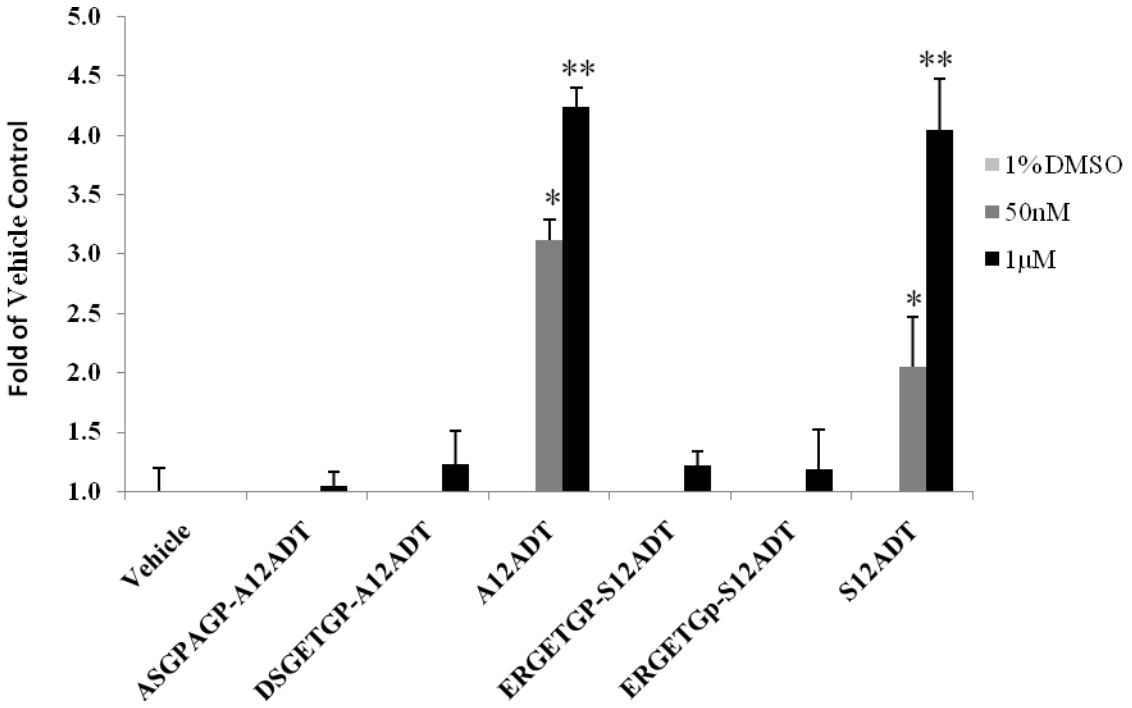

Figure 2: Differential Ability to Elevated Intracellular Calcium Concentrations by Active and Pro- forms of the Drugs
Prodrugs or their corresponding activity moieties were incubated with viable TSU cells in suspension. Intracellular calcium concentrations were monitored using a cell permeable calcium dye, Fura-2, AM, and

monitoring the excitation ratio at 340nm vs 380nm with an emission wavelength of 510nm. Active forms of the drugs have a 40- to 60-fold greater ability to elevate intracellular calcium levels than their prodrug counterparts.

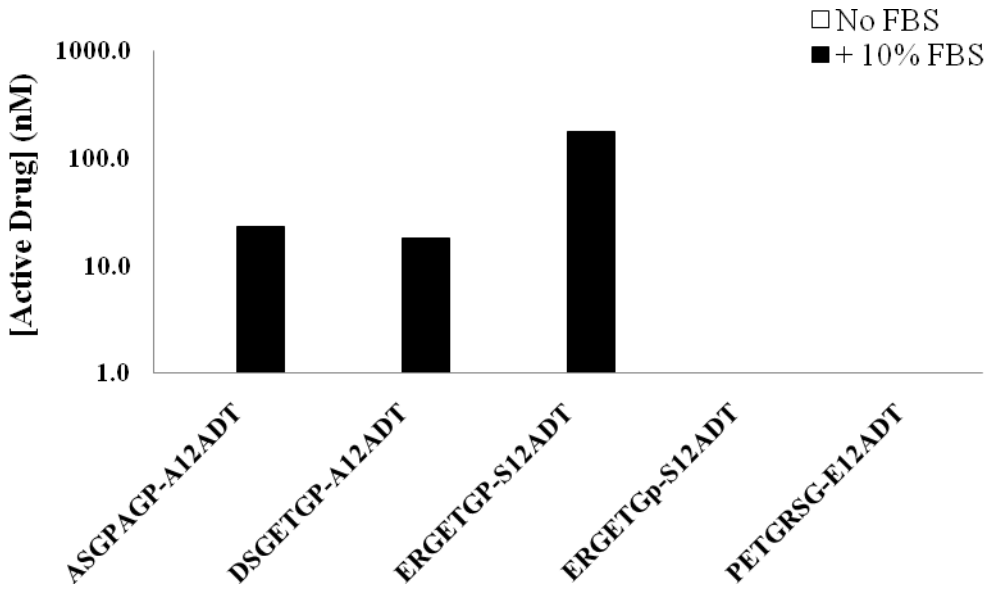

Figure 3: Release of the Active Drug from FAP Prodrugs in Tissue Culture Media supplemented with 10% FBS

Prodrugs ([100µM]) were incubated in DMEM +/- 10% FBS at 37°C for 24h. Free drug concentrations (A/S-12ADT) were determined by LCMS.

A.

Normal Rabbit IgG **Rb anti-mFAP pAb**

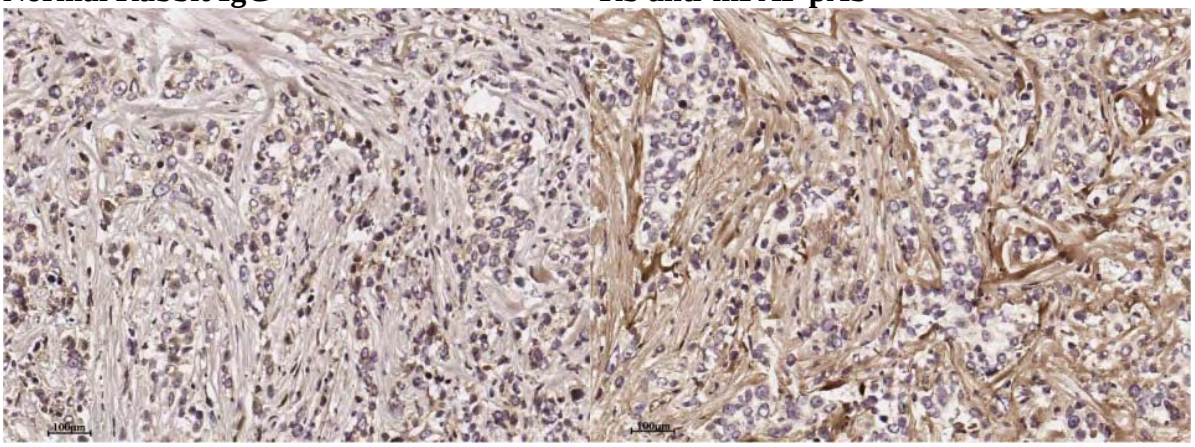

B.

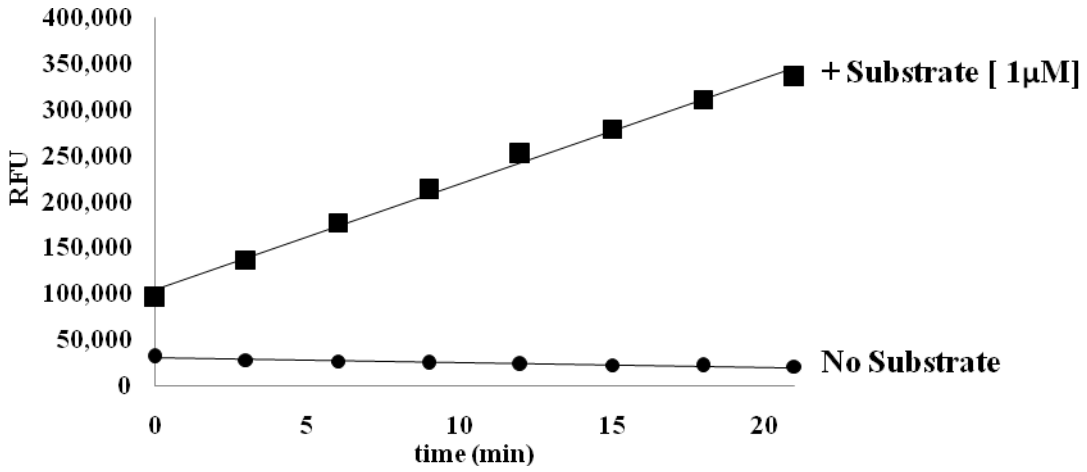

C.

FAP/αSMA **Vimentin/αSMA**

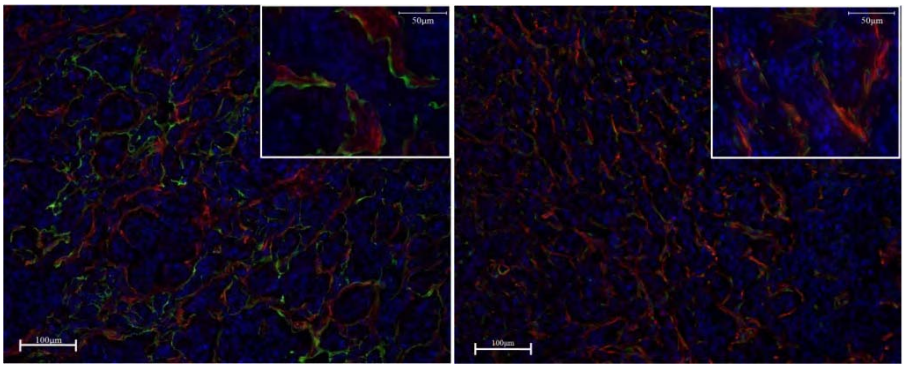

Figure 4: MCF-7 Xenografts as a Model to Evaluate FAP-activated Prodrugs

(A) FAP is expressed on mouse stromal cells in MCF-7 xenografts. Tumor sections were stained with a rabbit polyclonal anti-mouse FAP antibody (left panel) or normal rabbit IgG (right panel). Images are representative and were taken at 10x magnification. **(B)** Presence of FAP enzymatic activity in MCF-7 tumor homogenates as indicated by the hydrolysis of a FAP-selective fluorescence-quenched peptide substrate (MCa-DRGETGPA-Dnp). **(C)** Fibroblasts infiltrating MCF-7 xenografts take on a reactive phenotype as characterized by the co-expression of FAP (left panel) or Vimentin (right panel) (green) & alpha-smooth muscle actin (red). Images are representative and were taken at 20x magnification. Insets are at 40x magnification.

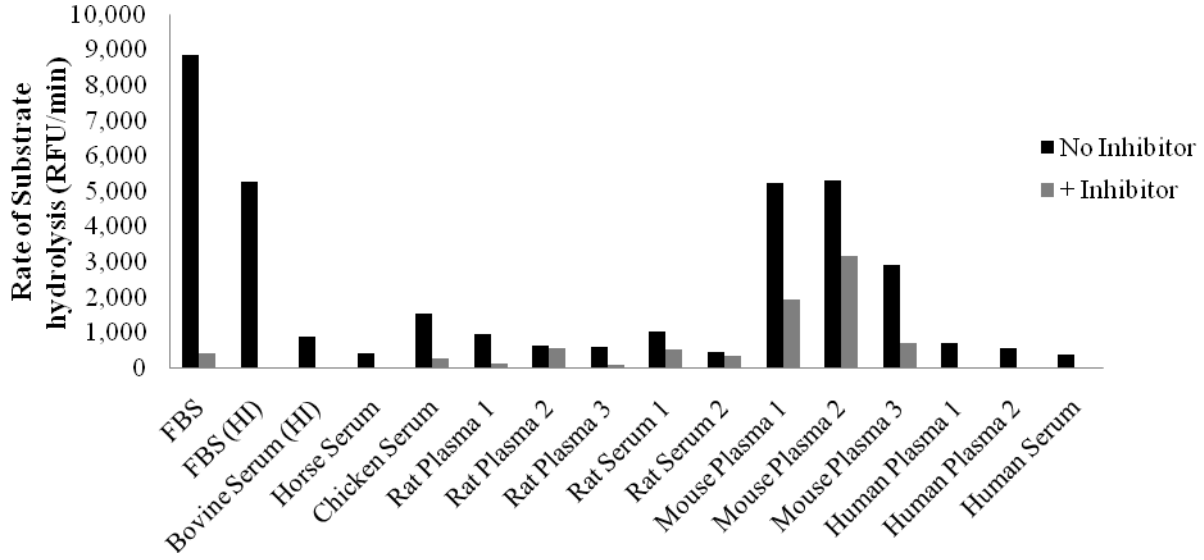

Figure 5: Comparison of FAP Enzymatic Activity in Plasma/Serum from Multiple Species
Rate of MCa-ASGPAGPA-Dnp hydrolysis was measured at a substrate concentration of [20µM] +/- Inhibitor (AcGbP) at a concentration of [200µM].

A.

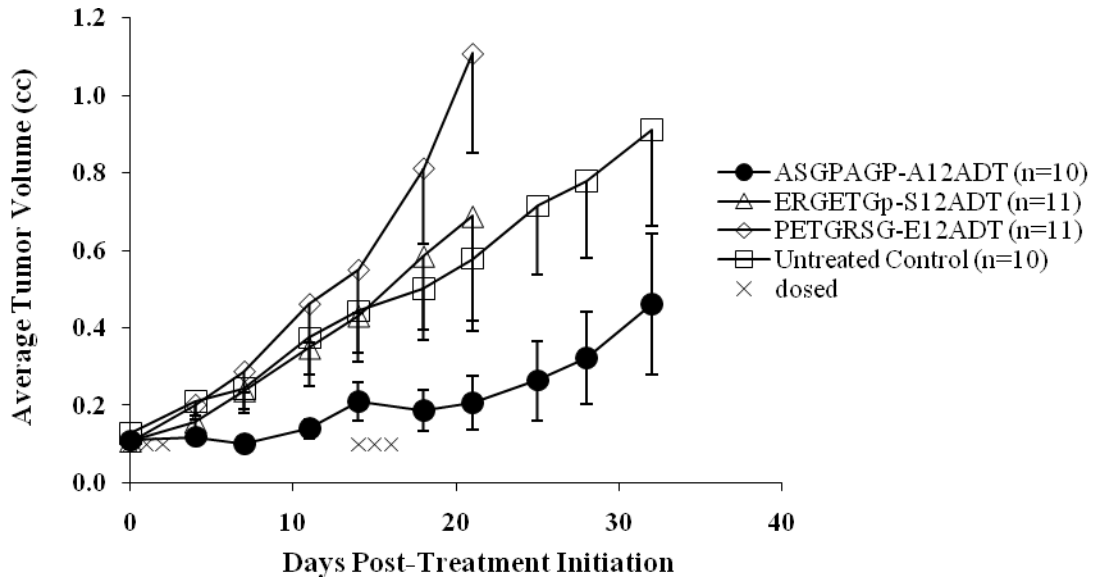

B.

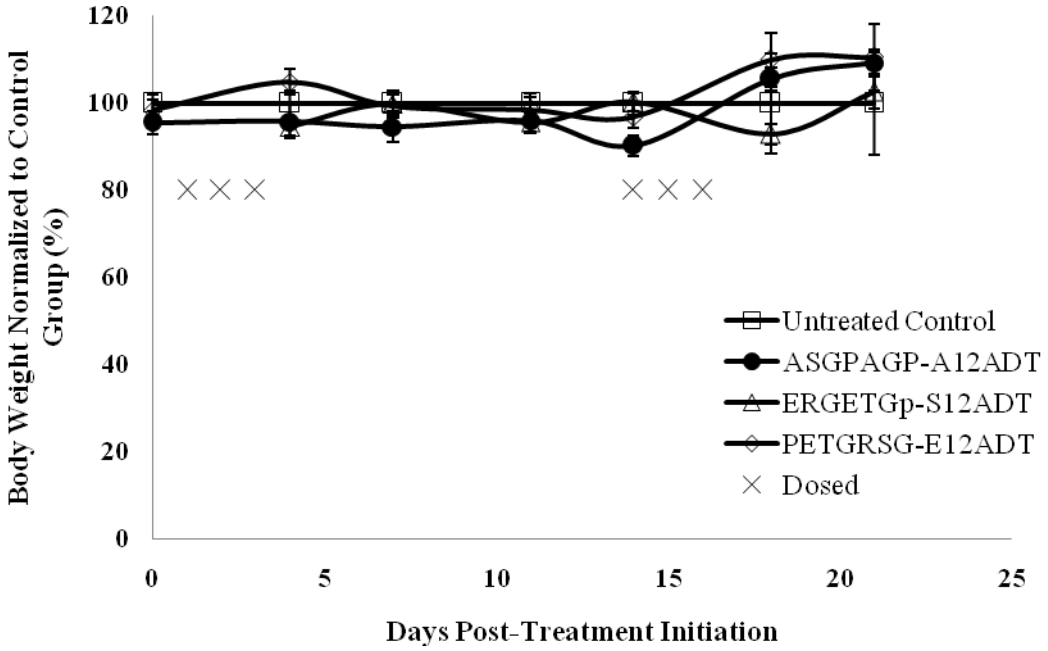
Body Weight Normalized to Control Group (%)
120
100
80
60
40
20
0
0
5
10
15
20
25
Days Post-Treatment Initiation
Untreated Control
ASGPAGP-A12ADT
ERGETGp-S12ADT
PETGRSG-E12ADT
Dosed

C.

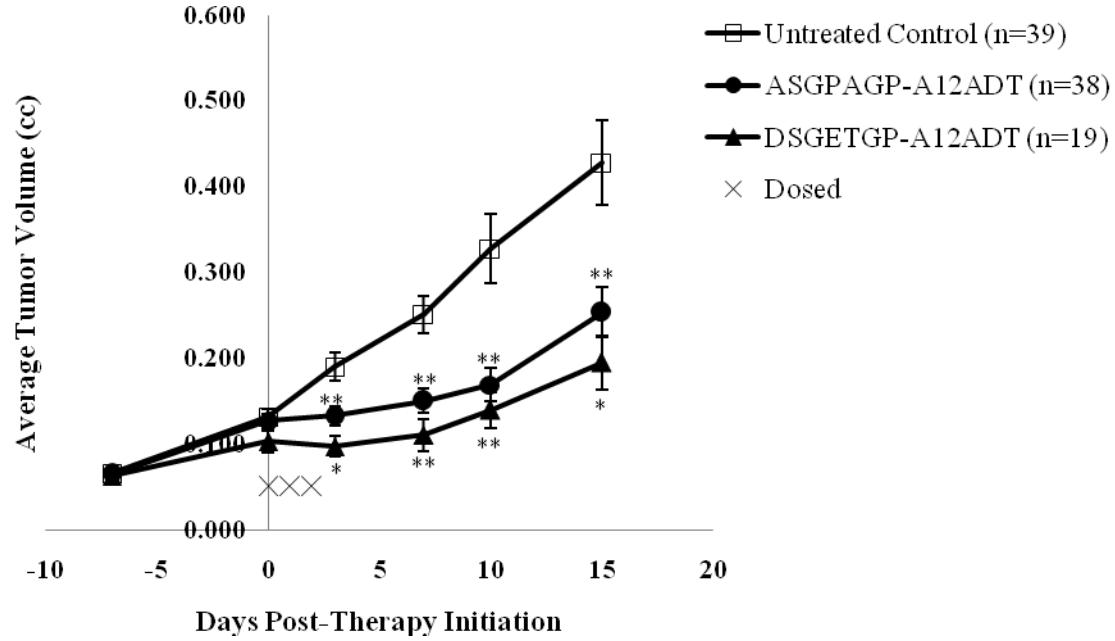
Average Tumor Volume (cc)
0.600
0.500
0.400
0.300
0.200
0.100
0.000
-10
-5
0
5
10
15
20
Days Post-Therapy Initiation
Untreated Control (n=39)
ASGPAGP-A12ADT (n=38)
DSGETGP-A12ADT (n=19)
Dosed
**
**
**
**
**
*
*

D.

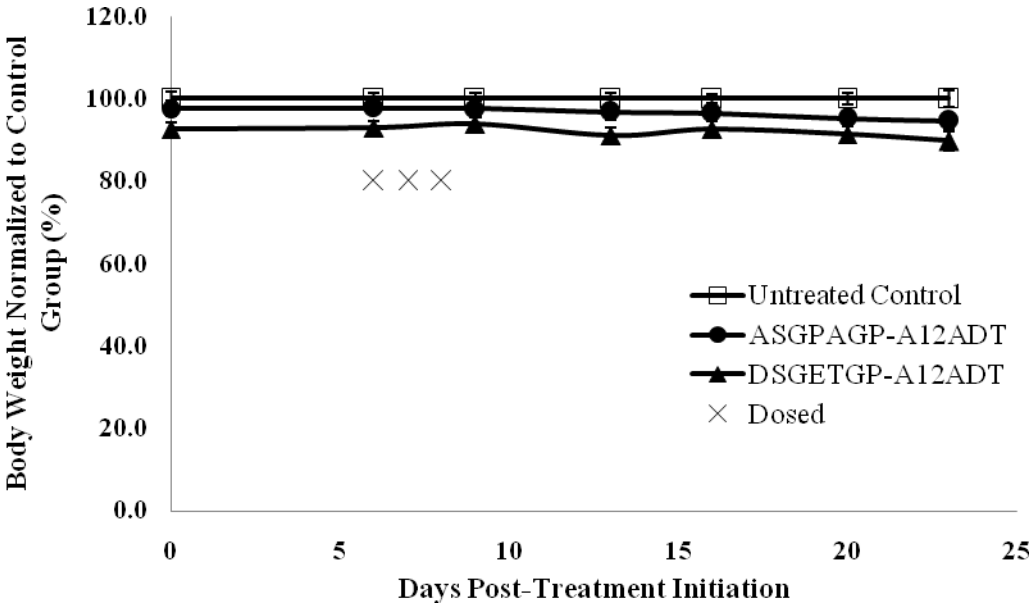

E.

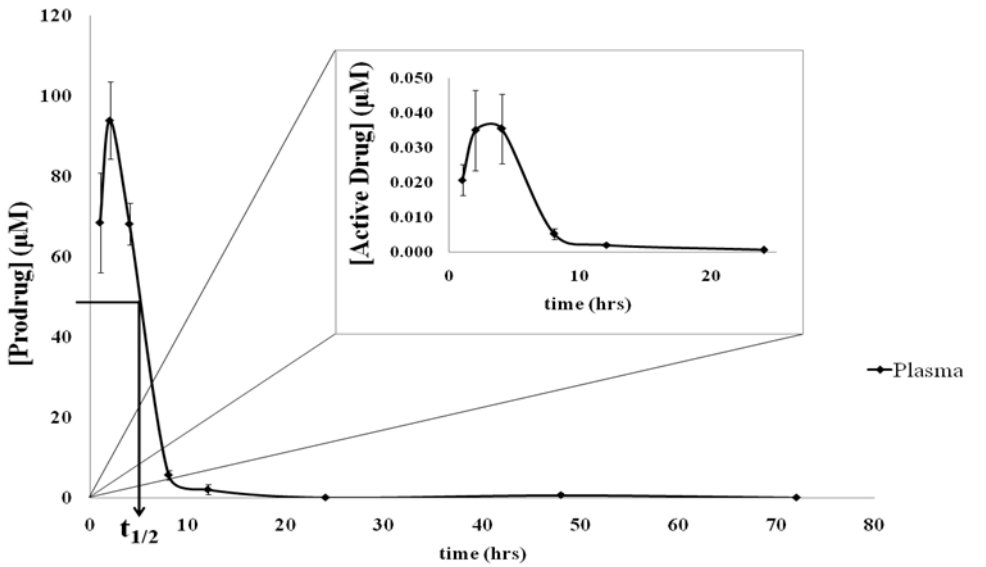

Figure 6: Anti-Tumor Efficacy of FAP-Activated Prodrugs vs MCF-7 Xenograft

(A) Mice bearing MCF-7 xenografts were treated IV with 100nmoles of either a FAP-activated prodrug (ASGPAGP-A12ADT) or one of two control prodrugs (ERGETGp-S12ADT or PETGRSG-E12ADT) and compared to untreated control tumors. Treatment regimen consisted of two courses of 3 consecutive daily doses with a 2wk recovery period between courses. Each group contained 10-11 mice and error bars represent +/- standard error. **(B)** Weight loss by treatment group in mice bearing MCF-7 xenografts from Fig. 6A normalized to the weight of the animals in the untreated control group. Weight loss in the treated animals did not significantly deviate from controls as defined by a change in weight greater than 10%. **(C)** Mice bearing MCF-7 xenografts were treated IV with 100nmoles of a FAP-activated prodrug (ASGPAGP-A12ADT or DSGETGP-A12ADT) and compared to untreated control tumors. Treatment regimen consisted of one courses of 3 consecutive daily doses. This is the averaged data from 4 independent experiments with ~10 mice/group/experiment. Error bars represent +/- standard error. Significance was determined using a two-sided

T-Test, where (*) represents a p-value < 0.05 and (**) represents a p-value < 0.01. **(D)** Weight loss by treatment group in mice bearing MCF-7 xenografts from Fig. 1C normalized to the weight of the animals in the untreated control group. Weight loss in the treated animals did not significantly deviate from controls as defined by a change in weight greater than 10%. **(E)** Half-life ($t_{1/2}$) of ASGPAGP-A12ADT in mouse plasma was determined to be ~5.3hrs with no accumulation of the prodrug seen at 24hrs following the second and third doses. Inset shows activation of the prodrug in mouse plasma in vivo represents less than <0.1% of the total amount given and is cleared rapidly.

A.

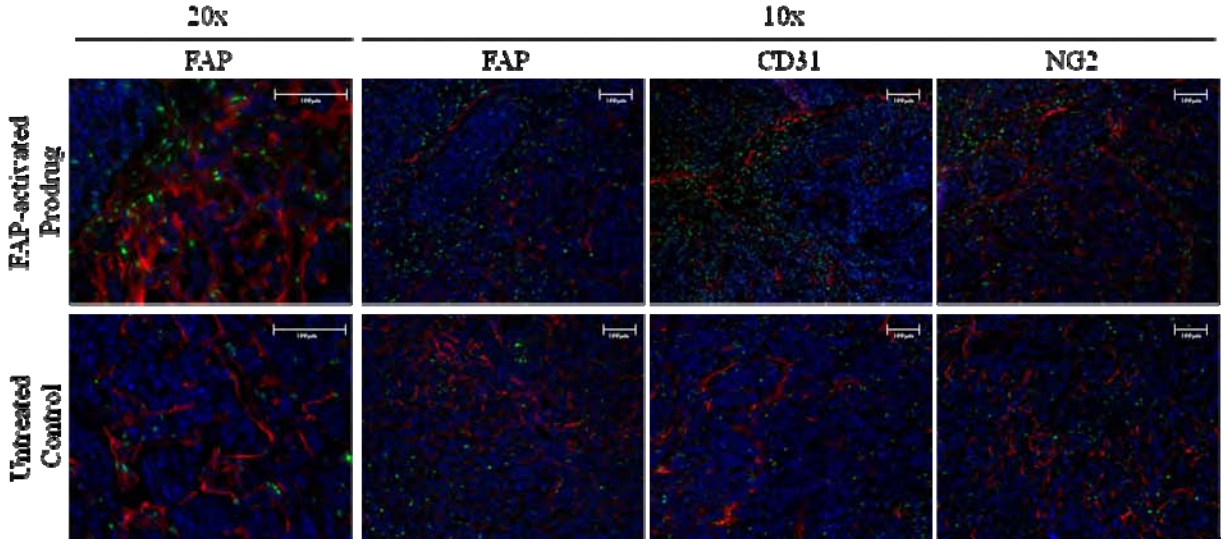

B.

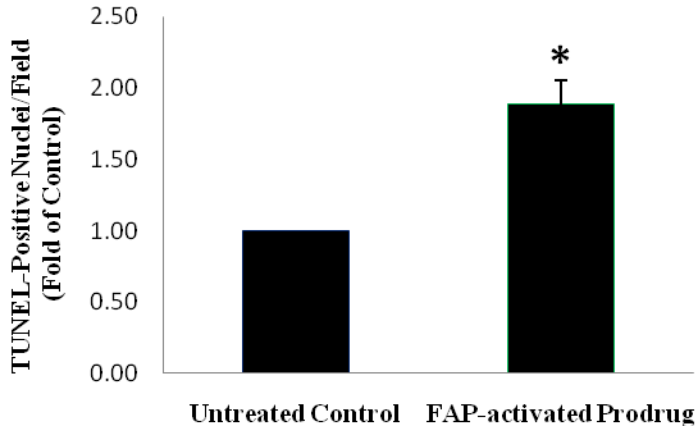

C.

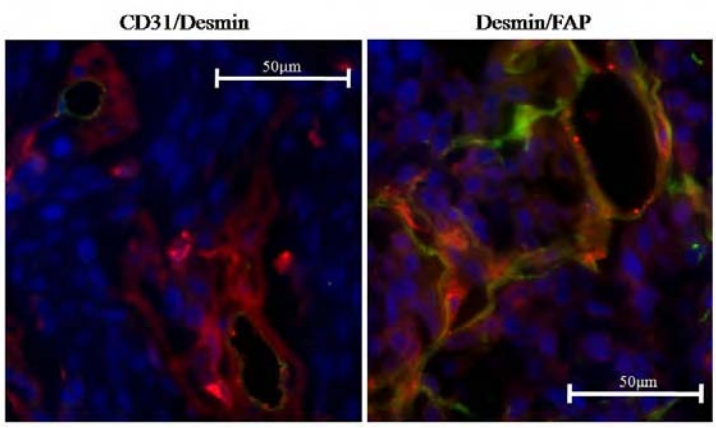
CD31/Desmin
Desmin/FAP
50μm
50μm

D.

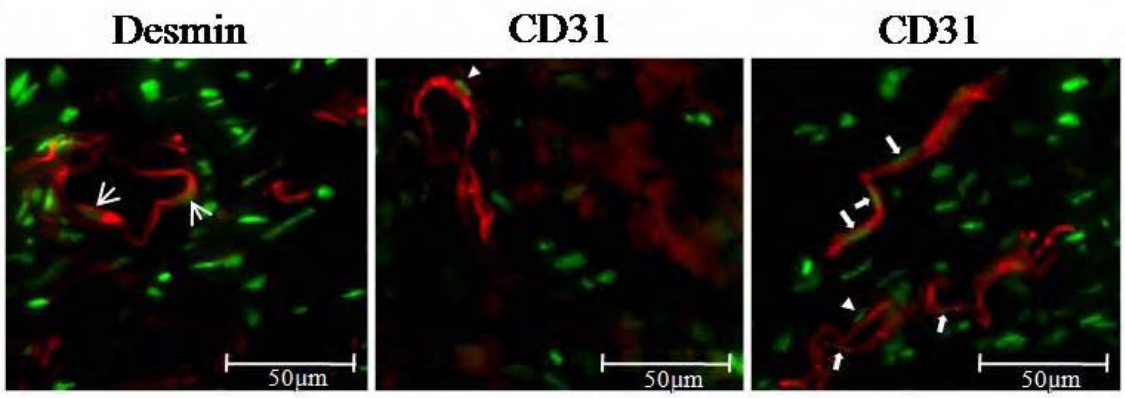
Desmin
CD31
CD31
50μm
50μm
50μm

E.

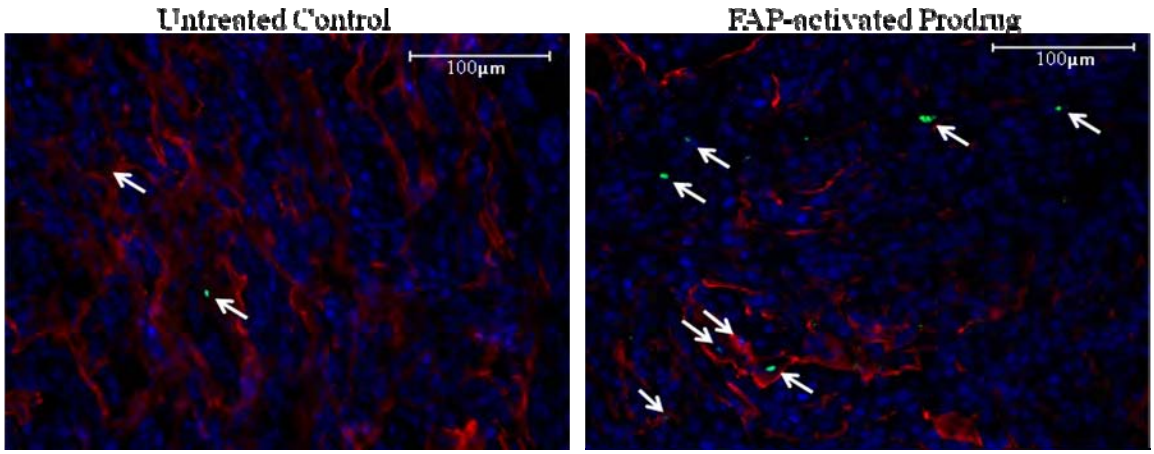
Untreated Control
FAP-activated Prodrug
100μm
100μm

F.

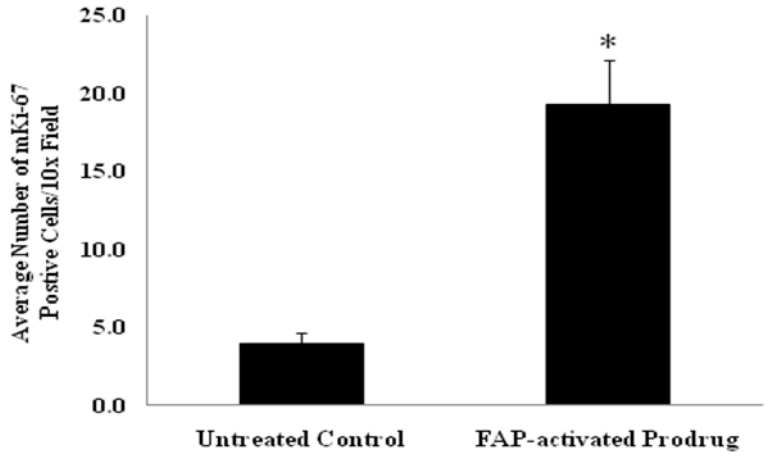

Figure 7: Stromal-selective cell death in tumors treated with FAP-activated prodrugs

(A) Stromal cells (red) (CAFs – FAP (Left), Endothelial Cells – CD31 (Middle), Pericytes – NG2 (Right)) selectively undergo apoptosis designated by TUNEL-positive (green) nuclei following treatment with a FAP-activated prodrug, whereas untreated control tumors show a more general pattern of cell death. Nuclei are counterstained with DAPI (blue). Images are representative of 3 images/tumor and 3 tumors/group. Images were taken at both 10x and 20x magnifications. **(B)** Quantification of TUNEL staining from images represented in panel A. Average of 9 images/group. Error bars represent + Standard Error and the (*) represents a p-value = 0.0008 calculated by a two-sided T-Test. **(C)** (Left Panel) CD31-positive (green) vascualar endothelial cells are associated with Desmin-positive pericytes (red). Nuclei are counterstained with DAPI (blue). Images taken at 40x magnification. **(D)** Vascular endothelial cells and pericytes undergo apoptosis in MCF-7 xenografts treated with a FAP-activated prodrug. (Left Panel) Desmin-positive (Red) pericytes with TUNEL-positive (green) nuclei (arrow). (Middle Panel) Perivascular cells (arrowhead) with TUNEL-positive (green) nuclei associated with a CD31-positive (Red) blood vessel. (Right Panel) CD31-positive (Red) endothelial cells with TUNEL-positive (green) nuclei (block arrow) as the result of a bystander effect from prodrug targeting. Nuclei are counterstained in all images with DAPI (blue). Images taken at 40x magnification. **(E)** Stromal cells in areas of FAP (red) expression begin to proliferate (mKi-67-positive – green, arrowhead) following treatment with a FAP-activated prodrug. Nuclei are counterstained with DAPI (blue). Images are representative of 6 images/tumor and 3 tumors/group. Images were taken at both 20x and 10x magnifications. **(F)** Quanitification of mouse stromal cell proliferation in MCF-7 xenografts from images represented in panel E. Average of 9 images/group. Error bars represent + Standard Error and the (*) represents a p-value = 0.00002 calculated by a two-sided T-Test.

	Compound	IC_{50} ([nM] +/- SE)
Active Drug	12ADT	2.8 +/- 0.24
	A12ADT	2.9 +/- 0.05
	S12ADT	3.5 +/- 0.13
	E12ADT	1.9 +/- 0.22
Prodrug	ASGPAGP-A12ADT	3.5 +/- 0.04
	DSGETGP-A12ADT	3.4 +/- 0.11
	ERGETGP-S12ADT	3.4 +/- 0.14
	ERGETGp-S12ADT	>1000
	PETGRSG-E12ADT	>1000

Table 1: Efficacy of FAP-Activated Prodrugs vs. MCF-7 breast cancer cell line *in vitro*

	Surviving Fraction (# of Consecutive Daily Doses)				
Compound	**1nmole**	**10nmoles**	**100nmoles**	**300nmoles**	**1000nmoles**
ASGPAGP-A12ADT	--	--	3/3 (3)	3/3 (2) 0/3 (3)	0/3 (1)
DSGETGP-A12ADT	--	--	3/3 (3)	3/3 (2) 0/3 (3)	0/3 (1)
ERGETGP-S12ADT	--	--	3/3 (3)	3/3 (2) 0/3 (3)	0/3 (1)
ERGETGp-S12ADT	--	--	3/3 (3)	3/3 (2) 0/3 (3)	0/3 (1)
PETGRSG-E12ADT	--	--	3/3 (3)	3/3 (2) 0/3 (3)	0/3 (1)
A12ADT	3/3 (3)	0/3 (1)	0/3 (1)	--	--

Table 2: Maximum tolerated dose (MTD) of FAP-activated prodrugs.
The number of mice surviving each dosing level is listed as a fraction of the total number of mice dosed at that level. The number of consecutive daily doses given at each level is listed in parentheses.

Fibroblast Activation Protein Peptide Substrates Identified from Human Collagen I Derived Gelatin Cleavage Sites†

Saurabh Aggarwal,‡,§ W. Nathaniel Brennen,|| Thomas P. Kole,|| Elizabeth Schneider,‡ Ozlem Topaloglu,‡ Melinda Yates,|| Robert J. Cotter,|| and Samuel R. Denmeade*,‡,§,||

The Sidney Kimmel Comprehensive Cancer Center at Johns Hopkins, Chemical and Biomolecular Engineering Department, and Department of Pharmacology and Molecular Sciences, The Johns Hopkins University, Baltimore Maryland 21231

Received September 20, 2007; Revised Manuscript Received November 26, 2007

ABSTRACT: A highly consistent trait of tumor stromal fibroblasts is the induction of the membrane-bound serine protease fibroblast activation protein-α (FAP), which is overexpressed on the surface of reactive stromal fibroblasts present within the stroma of the majority of human epithelial tumors. In contrast, FAP is not expressed by tumor epithelial cells or by fibroblasts or other cell types in normal tissues. The proteolytic activity of FAP, therefore, represents a potential pan-tumor target that can be exploited for the release of potent cytotoxins from inactive prodrugs consisting of an FAP peptide substrate coupled to a cytotoxin. To identify FAP peptide substrates, we used liquid chromatography tandem mass spectroscopy based sequencing to generate a complete map of the FAP cleavage sites within human collagen I derived gelatin. Positional analysis of the frequency of each amino acid at each position within the cleavage sites revealed FAP consensus sequences PPGP and (D/E)-(R/K)-G-(E/D)-(T/S)-G-P. These studies further demonstrated that ranking cleavage sites based on the magnitude of the LC/MS/MS extracted ion current predicted FAP substrates that were cleaved with highest efficiency. Fluorescence-quenched peptides were synthesized on the basis of the cleavage sites with the highest ion current rankings, and kinetic parameters for FAP hydrolysis were determined. The substrate DRGETGP, which corresponded to the consensus sequence, had the lowest K_m of 21 μM. Overall the K_m values were relatively similar for both high and low ranked substrates, whereas the k_{cat} values differed by up to 100-fold. On the basis of these results, the FAP consensus sequences are currently being evaluated as FAP-selective peptide carriers for incorporation into FAP-activated prodrugs.

The growth of epithelial neoplasms requires the formation of a supporting tumor stroma to supply nutrients and growth factors for tumor cell survival and continued growth. This invasive growth is associated with characteristic changes in the supporting stroma that include induction of tumor blood vessel formation, the recruitment of reactive stromal myofibroblasts, lymphocytes, and macrophages, the release of peptide signaling molecules and proteases, and the production of an altered extracellular matrix (*1*−*5*). The tumor stroma compartment represents a major component of the mass of most carcinomas, with 20−50% commonly seen in breast, lung, and colorectal cancers and reaching >90% in carcinomas that have desmoplastic reactions such as breast and pancreatic cancers (*5*, *6*).

Unlike malignant epithelial cells, activated tumor stromal fibroblasts are not transformed genetically and do not demonstrate the genetic and phenotypic heterogeneity seen in malignant cells. Reactive tumor stromal fibroblasts differ from fibroblasts of normal adult tissues in regard to morphology, gene expression profiles, and production of important biological mediators such as growth factors and proteases (*1*, *6*, *7*). For example, a highly consistent trait of tumor stromal fibroblasts is the induction of fibroblast activation protein-α (FAP).[1] FAP was originally identified as an inducible antigen expressed on reactive stroma and given the name "fibroblast activation protein". FAP was independently identified by a second group as a gelatinase expressed by aggressive melanoma cell lines and was given the name "seprase" for surface-expressed protease (*8*). Subsequent cloning of FAP and seprase revealed that they are the same cell-surface serine protease.

FAP was originally reported to be a cell-surface antigen recognized on human astrocytes and sarcoma cell lines in vitro by the F19 monoclonal antibody (MAb) (*9*). In one series using human tissues, FAP was detected in the stroma of over 90% of malignant breast, colorectal, skin, and

† This work supported by funding from the Susan G. Komen Breast Cancer Foundation (to S.R.D.), the Department of Defense Breast Cancer Research Program (Grant DAMD17-03-1-0304) (to S.R.D.), and a Department of Defense Prostate Cancer Research Program Pre-Doctoral Award (to W.N.B.). The Mass Spectrometry/Proteomics Facility at the Johns Hopkins University School of Medicine is supported by NCRR Grant 1S10-RR14702, the Johns Hopkins Fund for Medical Discovery, and the Institute for Cell.

* To whom correspondence should be addressed. Phone: (410) 502-3941. Fax: (410) 614-8397. E-mail:denmesa@jhmi.edu.

‡ The Sidney Kimmel Comprehensive Cancer Center at Johns Hopkins.

§ Chemical and Biomolecular Engineering Department.

|| Department of Pharmacology and Molecular Sciences.

[1] Abbreviations: FAP, fibroblast activation protein; LC/MS/MS, liquid chromatography/tandem mass spectrometry; MALDI-TOF, matrix-assisted laser desorption/ionization time of flight; Mca, 7-methoxycoumarin-4-acetic acid; Dnp, dinitrophenyl.

10.1021/bi701921b CCC: $40.75
Published on Web 12/21/2007 PAGE EST: 10.1

pancreatic tumors (*7*, *10*). In contrast, most normal adult tissues have demonstrated no detectable FAP protein expression (*7*). FAP expression has been most characterized in breast tissue. Garin-Chesa et al. used the F19 MAb to demonstrate strong (12/14) and moderate (2/14) expression of FAP in the stroma of human breast carcinomas but observed no expression by breast cancer epithelial cells and no expression in adjacent normal breast tissue. Additionally, little to no expression was observed in the stroma or epithelial cells of 10/10 samples of fibrocystic disease and 2/2 samples of fibroadenomas (*7*).

FAP is a member of the enzyme class known as post-prolyl peptidases that are uniquely capable of cleaving the Pro−X amino acid bond. These enzymes have been demonstrated to play a role in cancer biology and are capable of modifying bioactive peptides (*11*). This group of proteases includes the well-characterized dipeptidyl peptidase IV (DPPIV) as well as DPPII, DPP6, DPP7, DPP8, DPP9, prolyl carboxypeptidase, and prolyl endopeptidase (*11*). The substrate preferences for many of these prolyl peptidases are not entirely known, but like DPPIV, they all have dipeptidase functionality. FAP is highly homologous to DPPIV (*11*). Like DPPIV, FAP is a type II integral membrane protein that is able to cleave peptides with proline as the penultimate amino acid (*12*). However, FAP differs from DPPIV in that it also has gelatinase and, possibly, collagenase activity (*8*, *11*). Using zymography, FAP was demonstrated to cleave gelatin and human collagen I but was unable to cleave human fibronectin, laminin, or collagen IV (*12*). These results suggest that FAP's physiologic function may be primarily that of an endopeptidase that can degrade proteins rather than a dipeptidase like DPPIV. This additional gelatinase/collagenase activity may be unique to FAP among the family of prolyl proteases. Unlike DPPIV, FAP is also not widely expressed in most normal tissues (*11*).

Our laboratory has been engaged in the development of prodrugs that can be selectively activated by tissue-specific proteases (*13*−*17*). These prodrugs are produced by coupling a cytotoxic agent to a peptide carrier to produce an inactive compound that can only become activated upon release of the cytotoxin from the peptide by proteolysis. Our initial efforts have focused on the development of prodrugs activated by the prostate cancer serine proteases prostate-specific antigen (PSA) and human glandular kallikrein 2 (hK2) that are both members of the kallikrein family (*13*−*16*). In contrast to this tissue-specific approach, FAP represents a potential pan-tumor target. To develop FAP-activated prodrugs requires the identification of a peptide substrate that is selectively hydrolyzed by FAP. In the current study, we present results using liquid chromatography/tandem mass spectrometry (LC/MS/MS) to generate a complete map of FAP cleavage sites within recombinant forms of human collagen I derived gelatin. We have synthesized selected peptides on the basis of these cleavage maps and analyzed them for hydrolysis by FAP to identify peptides that could be used to target cytotoxins to FAP-expressing tumor tissue.

EXPERIMENTAL PROCEDURES

Materials. The *Drosophila* Expression System (DES) was from Invitrogen (Rockville, MD). Peptide Ala-Pro-AFC [AFC = 7-amino-4-(trifluoromethyl)coumarin] was from Bachem (Heidelberg, Germany). Gly-Pro-AMC, the MMP substrate sampler kit, and all other peptide synthesis reagents were from Anaspec (San Jose, CA). Novatag Dnp resin, *N*-(7-methoxycoumarin-4-acetyloxy)succinimide (Mca-Osu), 1-hydroxybenzotriazole (HOBt), and *N*-methyl-2-pyrrolidone (NMP) were from Novabiochem, San Diego, CA. Unless otherwise indicated all the other reagents were from Sigma-Aldrich (St. Louis, MO).

FAP Cloning and Expression. A PCR approach was used to amplify and attach a His_6 tag to the amino terminus of the extracellular domain of FAP (Genbank accession number NM_004460). The primers used were (forward *Bgl*II) 5′-GGAAGATCTCATCATCACCATCACCATCGCCCTTCAAG-3′ and (reverse *Xho*I) 5′-GGCCTCGAGTCATTAGTCTGACAAAGAGAAACACTGC-3′. Template amplification was performed using *Pfu* polymerase (Promega, Madison) as per the suggested protocol. A PCR reaction began with an initial denaturation step (94 °C for 2 min) followed by three cycles of amplification (94 °C for 30 s, 40 °C for 1 min, 72 °C for 2 min), followed by 30 cycles of amplification (94 °C for 30 s, 58 °C for 1 min, 72 °C for 2 min), and ended with a final extension step (72 °C for 10 min). A 2 kb PCR fragment was purified by gel electrophoresis, digested with *Bgl*II/*Xho*I, and cloned into pMT/BiP/V5−HisA (Invitrogen, California) previously digested with the same set of enzymes. The final construct was designated as pMT−His−FAP.

Transfection of Insect Cells and Stable Cell Line Generation. Schneider's S2 cells (Invitrogen) were maintained in DES medium (Gibco, Rockville, MD) supplemented with 10% heat-inactivated fetal bovine serum (FBS) at room temperature. Before transfection, the cells were seeded in a 35 mm dish and grown until they reached a density of $(2-4) \times 10^6$ cells/mL. The cells were cotransfected with 19 μg of pMT−His−FAP and 1 μg of a pCoHYGRO selection vector using a kit for calcium phosphate-mediated transfection (Invitrogen). The calcium phosphate solution was removed 16 h post-transfection, and fresh DES medium supplemented with 10% FBS was added (a complete medium). The cells were grown for an additional 2 days, and then the medium was replaced with the complete medium containing 400 μg/mL hygromycin B (Invitrogen). The selection medium was changed every 3−4 days. Extensive cell death of nontransfected cells was evident after about 1 week, and cells resistant to hygromycin B started to grow out 2−3 weeks post-transfection.

His-Tagged FAP Large-Scale Expression and Purification. The hygromycin-resistant cells were seeded in 10 T-150's at a density of 1 million cells/mL. When the cells reached a density of 2−3 million cells/mL, 500 μM $CuSO_4$ was added to induce FAP expression. The cells were grown until they reached a density of 10−15 million cells/mL (8−9 days). A 2 mL portion of 200 mm L-glutamine was added to the cell suspension on days 2 and 6. Conditioned medium containing secreted FAP was collected after 12−14 days. The medium was concentrated, and excess $CuSO_4$ was removed by three rounds of ultrafiltration using an Amicon 8480 membrane (Millipore) with a 30 000 kDa cutoff. After each round of ultrafiltration, the volume was made up using sterile water. Final purification was obtained by incubating the concentrate with Ni−NTA resin (Qiagen, California) in manufacturer-recommended salt and imidazole concentrations. FAP was

eluted from the resin using 250 mM imidazole. The final 30 mL of eluate was diluted with water to 300 mL, and imidazole was removed by two rounds of ultrafiltration. The purity was checked by SDS−PAGE and Coomassie staining. Western blots were probed with anti-His tag [penta-His−horse radish peroxidase (HRP) conjugate from Qiagen). Overall, a yield of 1−2 mg was obtained from a 700 mL culture. Final purified aliquots were stored in reaction buffer at −20 °C.

FAP Enzyme Activity. FAP dipeptidyl peptidase activity was determined by digesting 500 μM Ala-Pro-AFC (Calbiochem) with rhFAP as described by Park et al. (*12*). Assays were performed at 23 °C in 100 mM Tris, 100 mM NaCl at pH 7.8 in 10% DMSO and 0.3% Brij-35. The fluorescence output was monitored every 30 s using a DTX 880 multimode detector (Beckman Dickinson). Standard curves of AFC (Calbiochem) fluorescence vs concentration were run with each assay to convert relative fluorescence units to moles of product generated. Excitation/emission wavelengths of 370 and 535 nm, respectively, were used to monitor liberation of the AFC fluorophore. The rate of hydrolysis (mol/min) was ascertained by determining the slope during the first minute of the reaction. This rate was then used to calculate the enzyme units per unit volume with 1 unit of enzyme activity being defined as the cleavage of 60 μmol of substrate/min.

FAP Gelatinase Assay. Quenched gelatin and collagen conjugates were used to detect and confirm FAP's gelatinase and collagenase activity. DQ gelatin from pig skin and DQ collagen type IV from human placenta fluorescence-quenched conjugates (Invitrogen, Rockville, MD) were digested with FAP, and digestion was monitored on a fluorescence plate reader. Protein substrates were dissolved in reaction buffer (100 mM NaCl, 100 mM Tris, pH 7.8) to a final concentration of 100 μg/mL. Trypsin digestion of each protein was used as a positive control. As a negative control the His-tagged extracellular domain of prostate-specific membrane antigen (PSMA), which was similarly purified from S2 cells under the same conditions as FAP, was also incubated with the quenched proteins. Fluorescence-quenched DQ bovine serum albumin (BSA) was used as a negative control for FAP protease activity.

Digestion of Recombinant Gelatin with FAP for Cleavage Mapping. Recombinant human gelatins of 100 and 8.5 kDa (Fibrogen, San Francisco, CA) were dissolved in reaction buffer, and 1 μg of FAP was added per 100 μg of protein substrate. Digestion was done for 4−6 h at 37 °C. As a positive control, trypsin digestion was performed. As a negative control, protein solutions were incubated with either BSA/buffer or buffer alone. Peptide fragments of size <30 kDa were purified using a 30 kDa Microcon spin filter (Millipore, Billerica, MA). The fragments were further purified with C_{18} spin tubes (Agilent, Palo Alto, CA) as per the suggested protocol with the substitution of 0.5% acetonitrile in place of 5% for binding and washing of the C_{18} columns. Samples were prepared for matrix-assisted laser desorption/ionization time of flight (MALDI-TOF) analysis on an Applied Biosystems Voyager-DE STR (mass accuracy ≥100 ppm) by 100:1 dilution with 2,5-dihydroxybenzoic acid (DHB) as the matrix. Analysis was performed in the linear mode over a mass acquisition range of 500−5000 Da with 50 laser shots performed per spectrum. Instrument calibration was performed routinely by the Mass Spectrometry Core Facility and was not performed prior to individual analyses.

Nanoflow HPLC and Mass Spectrometry. Peptides obtained from the FAP/gelatin digests were dried using a SpeedVac (Eppendorf), resuspended in LC/MS loading buffer (3% ACN, 0.1% formic acid), and analyzed using nanoflow LC/MS/MS on an Agilent 1100 series nano-LC system (Agilent) coupled to an LCQ DUO ion trap mass spectrometer (ThermoFinnigan). The LCQ was calibrated (*m*/*z* 50−2000) using the automatic calibration procedure outlined by the manufacturer. A fused silica capillary was loaded with a solution containing the Met-Arg-Phe-Ala (MRFA) peptide, caffeine, and Ultramark 1621 in 50% acetonitrile/0.1% formic acid. The capillary was connected to the nanoflow HPLC instrument and sprayed into the LCQ using the same flow rate and spray voltage used in all subsequent experiments. The calibration was tested using a standard 100 fmol tryptic digest of BSA and demonstrated a mass accuracy of ≤0.5 Da.

Peptides were preconcentrated on a 5 mm Zorbax C18 trap column (Agilent) and then eluted onto a 100 × 0.075 mm custom-packed Biobasic C18 (ThermoElectron) reversed-phase capillary column connected to a laser-pulled electrospray ionization emitter tip (New Objective) at a flow rate of 300 nL/min. Peptides were eluted from the nanospray source of the LCQ (Proxeon, Denmark) using the following gradient: 0% B at 0 min, 5% B at 8 min, 45% B at 50 min, 90% B at 55 min, 90% B at 60 min (solvent B is 0.1% formic acid in acetonitrile) at a spray voltage of 2.5 kV. The LCQ was operated in data-dependent mode using the Xcalibur software (ThermoFinnigan) in which every MS scan (400−1800 *m*/*z*) was followed by MS/MS scans (400−1800 *m*/*z*) on the three most intense ions using an isolation window of ±1.5 Da. Ions selected for MS/MS fragmentation were dynamically excluded for 30 s.

MS/MS data were searched against a collagen FASTA database using the SEQUEST search algorithm built into the Bioworks Browser (ThermoFinnigan), allowing for the variable modification of methionine oxidation. The peptides were initially filtered in a charge-dependent manner using an XCorr filter of 1.5, 2, and 2.5 for singly, doubly, and triply charged peptides. All MS/MS spectra used to identify peptides were manually inspected for validation of the y and b ion series. To quantify the relative abundance of each identified peptide, we compared the ion current for each of the observed peptide parent ions from the MS spectra. The contribution of each parent ion to the total ion current was extracted and integrated over the peptide elution peak.

Synthesis of Substrates Based on Determined Cleavage Sites. Quenched peptide substrates were prepared by using the 7-methoxycoumarin-4-acetic acid (Mca)/Dnp fluorophore/quencher pair. Synthesis of peptides was done using standard Fmoc solid-phase coupling on NovaTag Dnp resin with a substitution level of 0.4 mmol/g (Novabiochem, San Diego, CA). N-terminal capping was done twice overnight with Mca-Osu and HOBt in NMP. The peptides were cleaved with 95% TFA, 2.5% TIS, and 2.5% water. The purity and mass of each quenched peptide was confirmed by reversed-phase HPLC and MALDI-TOF analysis.

Protease Assays. The substrates were dissolved in DMSO at a stock concentration of 10 mM. Working concentrations of each substrate were made by making 2-fold dilutions

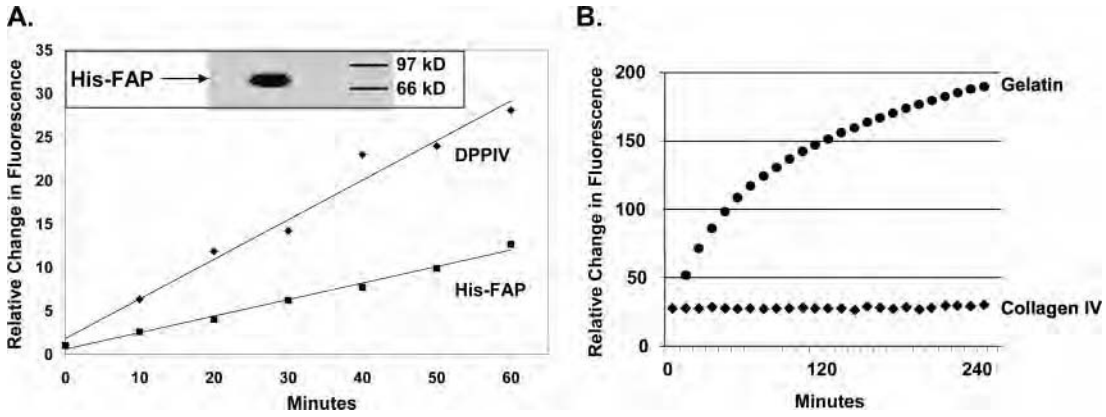

FIGURE 1: Characterization of recombinant His-tagged FAP. (A) Hydrolysis of the dipeptide substrate Ala-Pro-AFC (500 μM) by FAP (5 μg/mL) compared to DPPIV. The inset shows Western blot analysis of purified His−FAP following denaturing SDS−PAGE. (B) Digestion of indicated FITC-labeled proteins (100 μg/mL) by FAP (5 μg/mL).

ranging from 500 to 7.9 μM. rhFAP (10E−4 units, ~210−230 nM depending on the specific activity of the enzyme) was added to each assay where enzyme was included. The fluorescence of the cleavage product resulting from protease activity was monitored every 30 s using a DTX 880 multimode detector (Beckman Dickinson). Standard curves of Mca (Novabiochem) fluorescence vs concentration were run with each assay to convert relative fluorescence units to moles of product generated. Excitation and emission wavelengths of 340 and 435 nm, respectively, were used to monitor liberation of the Mca fluorophore peptide cleavage fragment. Assays were performed at 23 °C in 100 mM Tris, 100 mM NaCl at pH 7.8 in 10% DMSO and 0.3% Brij-35. Kinetic constants (K_m and k_{cat}) were calculated on the basis of the rate of hydrolysis (v) during the first minute of the reaction. Kinetic parameters were calculated from Michaelis−Menten plots (v vs [S]) with nonlinear regression analysis using SigmaPlot software.

RESULTS

Purification of Enzymatically Active FAP. The characterization of protease substrate specificity requires that the protease be of maximum purity and correctly folded to maintain enzymatic activity. Previously it had been shown that full-length FAP, cloned and expressed in *Drosophila* S2 cells, yielded highly pure protein that was enzymatically similar to the human form (*18*). Therefore, the extracellular domain of FAP was cloned with a His_6 tag at its N-terminus to generate a stable FAP-producing *Drosophila* S2 cell line. On induction with $CuSO_4$, FAP was secreted into the medium, which was then concentrated by ultrafiltration and purified using Ni−NTA beads. Purified FAP was demonstrated to be enzymatically active via its ability to cleave the dipeptide substrate Ala-Pro-AFC (*18*) (Figure 1A). Western blot analysis with an anti-His tag MAb documented the correct protein size of ~80 kDa (Figure 1A, inset).

Recombinant FAP Retains Gelatinase Activity. Quenched forms of gelatin and collagen were used to confirm the gelatinase and collagenase activity of recombinant FAP. Quenching is achieved by heavily labeling these proteins with the fluorophore FITC such that the fluorescence signal from the intact protein is minimal due to self-quenching by the fluorophore. Protein digestion releases FITC-labeled fragments that result in a measurable increase in overall fluorescence signal from the reaction mixture. Previously, it had been demonstrated using gel zymography that FAP can cleave gelatin and collagen I but could not cleave collagen IV (*12*). It remains unclear whether FAP can digest collagen I directly as recent studies suggest that the observed digestion may be due to an artifactual conversion of collagen I to gelatin during preparation (*12*, *19*, *20*). To confirm that our recombinant FAP maintained the ability to cleave gelatin, we used the FITC-quenched protein DQ gelatin from pig skin, with DQ collagen IV from human placenta serving as a negative control. In this assay, gelatin was readily hydrolyzed by FAP while collagen IV was not hydrolyzed (Figure 1B). MALDI-TOF analysis of the digested fragments was performed to confirm FAP hydrolysis. As a negative control, we demonstrated no digestion of any of the proteins using His-tagged human carboxypeptidase PSMA purified from *Drosophila* S2 cells under the same conditions (data not shown). These results confirm that gelatin hydrolysis was due to FAP and not due to the presence of some other protease contaminating our purification system.

MALDI for FAP Digest of Denatured Human Collagen I. To elucidate the substrate specificity of FAP, we examined FAP digests of unlabeled denatured human collagen I using MALDI-TOF mass spectrometry (Figure 2A). Digestion reactions were performed at a substrate to protease mass ratio of 200:1 using recombinant FAP or modified trypsin as a control. Two negative controls of collagen alone and FAP alone were also included to identify any peptides due to autolysis/degradation of these proteins. SDS−PAGE analysis of FAP-digested denatured collagen I (not shown) produced a smear of continuous size fragments, suggesting the presence of many cleavage sites. To simplify cleavage mapping by MALDI-TOF, small fragments (<5 kDa) were isolated by ultrafiltration and further purified using reversed-phase chromatography, Figure 2A. MALDI-TOF was subsequently performed using serial dilutions of the isolated peptides.

The masses of singly charged ions $[M + H]^+$ obtained from MALDI spectra were entered into the FindPept search tool at the ExPASy proteomics server (http://www.expasy-.org/tools/findpept.html) and used to perform a peptide mass fingerprint (PMF) search against the known collagen sequence. MALDI spectra suggest that denatured human collagen I is cleaved by FAP at numerous specific sites (Figure 2A); however, we were unable to unambiguously

A.

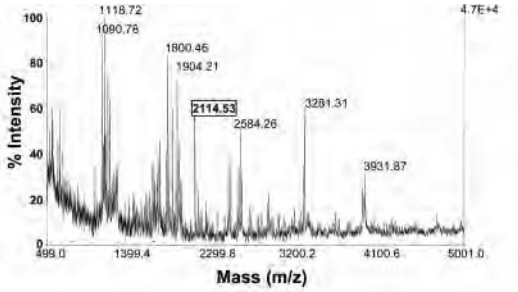

B.

FindPept Calculated Mass	Peptide Sequence	Position in FAP
2113.07	GAAGEPGKAGERGVPGPPGA VGPAG	55-79
2113.12	GPKGAAGEPGKAGERGVPGP PGAV	52-75
2113.12	PKGAAGEPGKAGERGVPGPP GAVG	53-76
2113.12	KGAAGEPGKAGERGVPGPPG AVGP	54-77
2113.12	AGEPGKAGERGVPGPPGAVG PAGK	57-80
2114.07	GRPGPPGPPGARGQAGVMGF PGP	31-53
2115.01	AVGPAGKDGEAGAQGPPGPA GPAGE	74-98

FIGURE 2: (A) MALDI-TOF mass spectra demonstrating FAP digestion of human collagen I. (B) Example of cleavage site sequence(s) determination using the FindPept tool for a selected mass of 2114.5 from MALDI-TOF mass spectra. Multiple potential cleavage site sequences within ±1 mass unit are identified by this analysis.

identify the cleavage sequences using the FindPept tool (Figure 2B). In most cases, multiple peptide sequences were matched for the same mass, and in some instances, more than 30 sequences were obtained for one particular mass. This result was most likely due to the fact that human collagen I is a heterotrimeric polymer made up of repeating sequences containing the $(GXY)_n$ motif (where X = Pro and Y = hydroxy-Pro). Human collagen I is also known to be glycosylated and cross-linked randomly throughout its sequence (*21*). These post-translational modifications in human collagen have not been well characterized and, therefore, make it more difficult to determine the exact cleavage sites using MALDI-TOF coupled with other proteomics tools. These results, while demonstrating that FAP cleaved denatured human collagen I, demonstrated the difficulties in obtaining correct cleavage sequences by mass spectrometry due to the polymeric nature and poorly defined qualities of human collagen I.

LC and Tandem MS/MS Analysis of FAP Digestion of Recombinant Gelatin. As collagen I derived gelatin is currently one of the only known protein substrates for FAP, we needed to develop an alternative method to identify FAP-selective cleavage sites within these proteins. To solve the problem of post-translational modification, we identified a source of recombinant human gelatin and collagen from FibroGen (South San Francisco, CA) that was prepared by cloning the human collagen I sequence in a strain of *Pichia pastoris* which lacks the enzyme prolyl hydroxylase (*22*). This human collagen I based gelatin is well characterized and has no post-translational modifications. This gelatin is used to produce drug capsules and vaccine adjuvants. Therefore, this recombinant gelatin was used in subsequent FAP cleavage mapping studies.

We next used MALDI-TOF to analyze FAP digestion of the 100 kDa recombinant form of human gelatin. SDS−PAGE separation and MALDI-TOF spectra showed that FAP readily digests the recombinant gelatin (data not shown). The masses of fragments <3 kDa were purified for MALDI-TOF spectra and again analyzed using the FindPept tool. However, once again multiple peptide sequences were obtained for each cleavage fragment.

A.

Cleavage Fragment			Theoretical [M+H]+	Charge	m/z (observed)
PPGAVGP/	AGK…AQGPPGP/	AGP	1308.62	2	654.81
-	GLP…SPGSPGP/	DGK	1449.77	2	725.39
KTGPPGP/	AGQ…PPGPPGA/	RGQ	1330.65	2	665.83
VMGFPGP/	KGA…PPGAVGP/	AGK	2113.12	2	1057.06
VMGFPGP/	KGA…GEPGKAG/	ERG	942.5	1	942.50
-	GLP…KTGPPGP/	AGQ	2256.16	2	1128.58
GFPGPKG/	AAG…PPGAVGP/	AGK	1928	2	964.50
FPGPKGA/	AGE…PPGAVGP/	AGK	1856.96	2	928.98
LTGSPGS/	PGP…KTGPPGP/	AGQ	1076.54	2	538.77
KTGPPGP/	AGQ…GPPGPPG/	ARG	1259.61	1	1259.61
VMGFPGP/	KGA…AGEPGKA/	GER	885.48	1	885.48
GLPGAKG/	LTG…SPGSPGP/	DGK	869.44	1	869.44
MGFPGPK/	GA- AGEPGKA/	GER	757.38	1	757.38
PGPPGAR/	GQA…VMGFPGP/	KGA	1017.48	1	1017.48
PGARGQA/	G- VMGFPGP/	KGA	761.37	1	761.37
GPPGPPG/	ARG…VMGFPGP/	KGA	1244.62	2	622.81
PPGPPGA/	RGQ…VMGFPGP/	KGA	1173.58	2	587.29
KTGPPGP/	AGQ…GARGQAG/	VMG	1799.89	2	900.45

B.

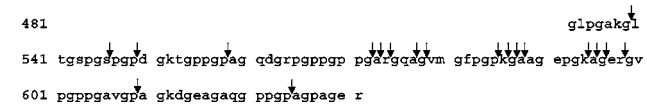

FIGURE 3: (A) FAP cleavage sites within the 8.5 kDa fragment of recombinant human collagen I derived gelatin. Cleavage sites are bracketed by "/", and $[M + H]^+$ denotes the mass of the cleavage fragment. Amino acids on the N-terminal side of the cleavage site (i.e., P7−P1) are in bold font. (B) Amino acid sequence of the 8.5 kDa fragment with FAP cleavage sites indicated by arrows.

Therefore, to resolve each particular mass fragment, an LC/MS/MS method was developed. To initially work out the methodological issues, peptide fragments from the FAP digest of the 8.5 kDa recombinant gelatin were time-resolved by nano-reversed-phase LC and then sequenced using an ion trap mass spectrometer operating in MS/MS mode (Figure 3A). MS/MS spectra were searched against the 8.5 kDa gelatin sequences using the SEQUEST algorithm with no cleavage specificity. In this analysis most of the identified cleavage sites occurred after proline. However, FAP cleavage sites in these gelatins were not restricted to proline alone. FAP was also found to cleave after Ala, Arg, Gly, Lys, and Ser. FAP was also able to cleave after multiple adjacent amino acids within the 8.5 kDa gelatin fragment (Figure 3B).

FAP Cleavage Map for Full-Length 100 kDa Gelatin. On the basis of the results with the 8.5 kDa gelatin fragment, we proceeded to use this LC/MS method to identify all of the FAP cleavage sites within the full-length 100 kDa recombinant gelatin. In an effort to identify the most preferentially cleaved sites, we also quantified the relative abundance of each of the identified peptides by integrating the ion current generated by each peptide throughout the chromatogram (Figure 4). After identification of a peptide from an MS/MS spectrum, we extracted the ion current for the parent mass of the ion from the total MS ion chromatogram using a 1.5 Da tolerance window and then integrated under the peak. In the case of multiple peaks, we chose the peak nearest to the retention time of the MS/MS spectrum matched to the peptide sequence of interest.

This analysis revealed a total of 51 FAP cleavage fragments within the 100 kDa recombinant gelatin (Figure 4). The corresponding fragment was mapped within the recombinant gelatin to determine the sequence of the amino acids upstream of the FAP cleavage site toward the N-

Cleavage Fragment		Theoretical $[M^+H]^+$	Charge	m/z (observed)	Extracted Ion Current
RTGDAGP/	VGP…PGPPGP	1373.72	1	1373.72	1.48E+11
ASGPAGP/	RGP…LNGLPGP/ IGP	1871.97	2	936.49	4.94E+10
DRGETGP/	AGP…APGAPGP/ VGP	1170.59	1	1170.59	2.34E+10
DRGETGP/	AGP…**DRGETGP/** AGP	2536.25	2	1268.63	2.15E+10
EPG**PPGP/**	AGF...DAG**PPGP/** AGP	2828.32	3	943.44	1.52E+10
RTGDAGP/	VGP…PGPPGPP/ GPP	871.47	1	871.47	1.47E+10
GETGPAG/	PPG…**DRGETGP/** AGP	2408.20	3	803.40	1.45E+10
QPSGPAG/	PTG…EPG**PPGP/** AGF	1742.86	2	871.93	1.31E+10
PSGPAGP/	TGA…EPG**PPGP/** AGF	1645.81	2	823.40	1.21E+10
PAGAAGP/	AGN…FPGARGP/ SGP	2812.39	2	1406.69	1.07E+10
PAGPPGA/	PGA…**DRGETGP/** AGP	2086.03	2	1043.52	9.34E+09
FQGLPGP/	AGP…DLGAPGP/ SGA	2112.04	2	1056.52	9.26E+09
MGFPGP/	KGA…PPGAVGP/ AGK	2113.12	2	1057.06	7.40E+09
PPGPAGP/	AGP…RVG**PPGP/** SGN	3556.85	3	1186.28	6.68E+09
RVG**PPGP/**	SGN…PPG**PPGP/** AGK	1004.48	1	1004.48	5.99E+09
AGRVGPP/	GPS…AGPPGPP / GPA	1004.48	1	1004.48	5.85E+09
PPGAPGP/	QGF…EPGASGP/ MGP	1665.75	1	1665.75	5.76E+09
ETGPAGP/	PGA…**DRGETGP/** AGP	2311.14	2	1156.07	4.82E+09
PPGAPGA/	PGA…**DRGETGP/** AGP	1860.92	2	930.96	4.39E+09
GLTGPIG/	PPG…**DKGESGP/** SGP	1390.66	2	695.83	4.22E+09
DRGETGP/	AGP…APGPVGP/ AGK	1423.73	1	1423.73	3.85E+09
ESGPSGP/	AGP…EPG**PPGP/** AGF	1870.92	2	935.96	3.34E+09
P**RGETGP/**	AGR...PPG**PPGP/** AGE	1341.69	2	671.35	3.31E+09
VRGLTGP/	IGP… **DKGESGP/** SGP	1560.77	1	1560.77	2.79E+09
PPGPTGP/	AGP…AKGEAGP/ QGP	1536.78	2	768.89	2.61E+09
FPGLPGP/	SGE…ERG**PPGP/** MGP	1905.91	2	953.45	2.18E+09
PPG**PPGP/**	AGE…APGTPGP/ QGI	1747.83	2	874.41	2.15E+09
LTGPIGP/	PGP…**DKGESGP/** SGP	1293.61	1	1293.61	2.11E+09
AKGDAGP/	AGP…GENGAPG/ QMG	1478.69	1	1478.69	1.48E+09
VMGFPGP/	KGA…AQGPPGP/ AGP	3402.72	3	1134.91	1.44E+09
PPGPAGA/	PG- **DKGESGP/** SGP	843.39	1	843.39	1.14E+09
PPGPMGP/	PGL…EGSPGRD/ GSP	2275.07	2	1138.04	1.06E+09
GFPGLPG/	PSG…ERG**PPGP/** MGP	2002.96	2	1001.98	1.01E+09
PPGPTGP/	AGP…EPG**PPGP/** AGA	3530.75	3	1177.58	9.13E+08
APGAPGA/	PGP…**DRGETGP/** AGP	1635.81	2	818.40	8.35E+08
PRGSEGP/	QGV…EPG**PPGP/** AGA	1147.59	1	1147.59	8.14E+08
TGDAGPV/	GP- PGPPGPP/ GPP	772.40	1	772.40	7.43E+08
GPAGFAG/	PPG… DAG**PPGP/** AGP	2425.14	3	809.05	6.91E+08
AKGEPGP/	VG- VQG**PPGP/** AGE	807.44	1	807.44	6.87E+08
AGPPGAD/	GQP…DAG**PPGP/** AGP	1987.95	2	994.47	5.43E+08
LPGPSGE/	PGK…ERG**PPGP/** MGP	1632.81	2	816.90	3.83E+08
GLTGPIG/	PPG…AGAPGDK/ GES	963.49	2	482.25	3.01E+08
KTG**PPGP/**	AGQ..GARGQAG/ VMG	1799.89	2	900.45	2.10E+08
GAKGDAG/	PPG…PAG PPG P/ IGN	1068.55	1	1068.55	1.59E+08
RGETGPA/	GPP…APGAPGP/ VGP	1099.55	1	1099.55	1.31E+08
ATGFPGA/	AG- RVGPPGP/ SGN	807.45	1	807.45	1.03E+08
PGPAGQD/	GRP...GARGQAG/ VMG	1428.75	2	714.87	7.53E+07
SGPRGLP/	G- PPGAPGP/ QGF	649.33	1	649.33	7.18E+07
PPGAVGP/	AGK AQG**PPGP/** AGP	1308.62	2	654.81	5.98E+07
AGPPGPA/	G- PAG**PPGP/** IGN	649.33	1	649.33	4.23E+07
PSGPQGP/	GGP…APGSKGD/ TGA	1819.86	2	910.43	3.58E+07

FIGURE 4: FAP cleavage sites within the 100 kDa recombinant human collagen I derived gelatin. Cleavage sites are bracketed by "/". The mass of the cleavage fragment, $[M + H]^+$, and extracted ion current are included for each cleavage site. Underlined sequences indicate cleavage sites which do not contain Pro (P) in the P1 position. The consensus sequences PPGP and D-(R/K)-G-E-(T/S)-G-P are indicated by bold text.

terminus. Since each fragment was produced by two cleavage events, 101 peptide sequences corresponding to the amino acids from P7 to P′1 could be mapped. Cleavage fragments were then ranked on the basis of the extracted ion current generated by each peptide (Figure 4). This ranking again revealed that FAP preferred to cleave after the G-P dipeptide. FAP was also able to cleave after other amino acids (i.e., Ala, Asp, Gly, Glu, Lys, and Val), but the majority of these cleavage fragments had very low extracted ion currents and were ranked in the lower half of the list (Figure 4). Often these non-proline cleavage sites were adjacent to a proline cleavage site. This result was also observed with the 8.5 kDa digest and suggested that the gelatin protein may misalign within the FAP catalytic site, resulting in low-level cleavage after non-proline amino acids.

On the basis of these cleavage sites, the frequency of individual amino acids within the P7−P′1 positions of each cleavage site was next determined. This analysis was somewhat limited by the repetitive nature of the collagen I sequence, and it was, therefore, not necessarily unexpected that the most frequent amino acids at each position were either proline or glycine, producing a consensus peptide with the sequence PPGPPGP. This exact sequence is found in 3 of the sequences within the map, while the peptide PPGP is found in 21 of the 101 sequences.

The frequency analysis, however, did reveal some additional trends that could bear on the identification of consensus sequences to be used in the development of FAP-activated peptide prodrugs (Figure 5). After proline in P7, for instance, the acidic amino acids Asp (23%) and Glu

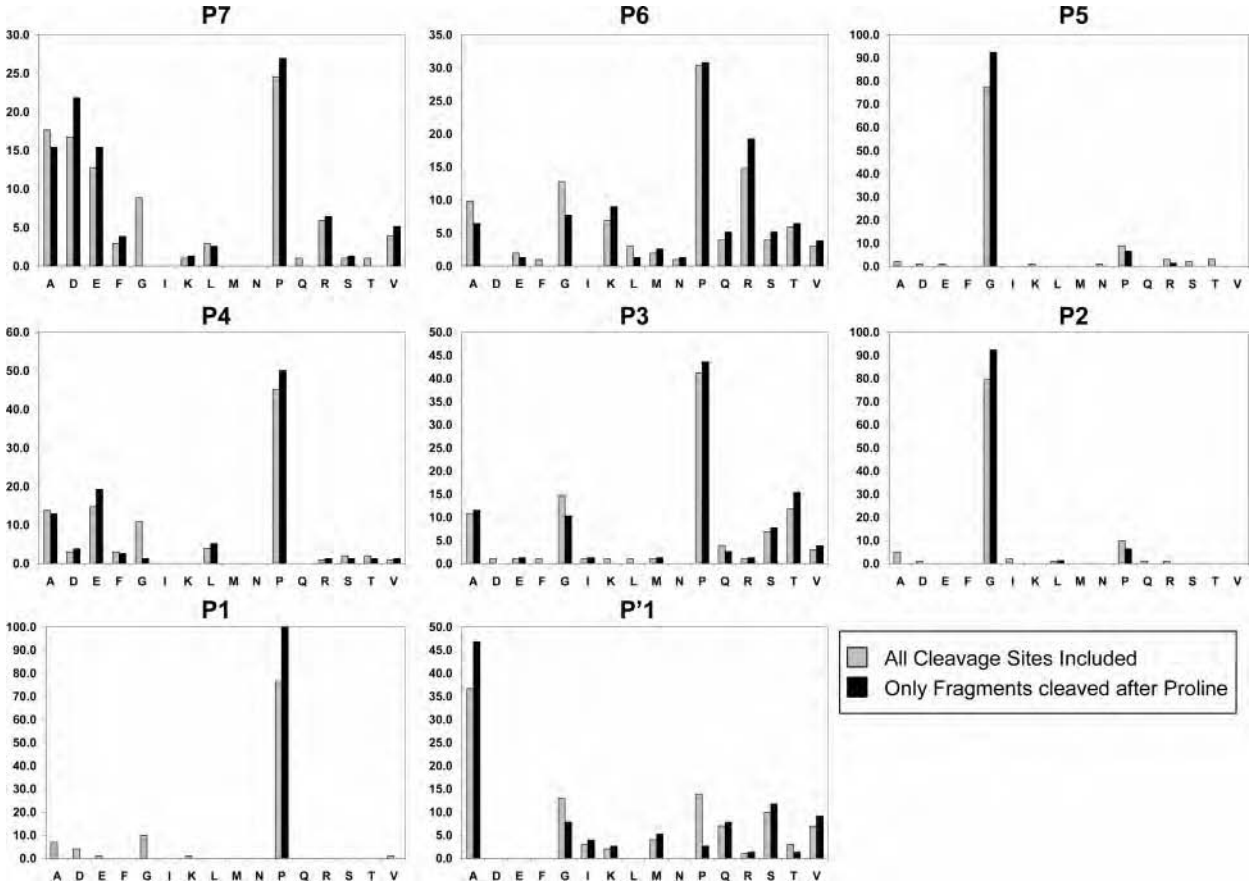

FIGURE 5: Frequency (%) of each amino acid in positions P7−P′1 within the FAP cleavage sites within the 100 kDa recombinant human collagen I derived gelatin. Gray bars indicate the frequency for all 101 cleavage sites. Black bars indicate the frequency in only those cleavage sites containing Pro (P) at the P1 position. The amino acids C, H, W, and Y are not present in human collagen I and, therefore, are not included.

Table 1: Frequency Analysis of Consensus Sequences within the 100 kDa Gelatin Amino Acid Sequence

amino acids								total no. of G-P cleavage sites[a] (%)	no. of FAP-cleaved sites[b] (%)
P7	P6	P5	P4	P3	P2	P1	P1′		
					G	P		116 (100)	40 (34)
					G	P	A	28 (24)	20 (71)
D/E	K/R	G	D/E	A/G/S/T	G	P		4 (3)	3 (75)
A/D/E/P	K/R	G	D/E/P	A/G/S/T/P	G	P		14 (12)	8 (57)
D/E	K/R/P	G	D/E/P	A/G/S/T/P	G	P		8 (7)	6 (75)
combined[c]								15 (13)	9 (60)
D/E/P	K/R/P	G	D/E/P	A/G/S/T/P	G	non-Pro		7 (6)	0 (0)

[a] Occurrence of the G-P dipeptide sequence in the 100 kDa gelatin sequence. [b] Number of times FAP cleaves after G-P sites. [c] Total unique sites from the consensus sequence indicated in rows 3−5.

(15%) were found in ~38% of the sequences. In P6, 30% of the sequences contained one of the basic amino acids Lys (10%) and Arg (20%). In P4, Glu was observed in 20% of the sequences and Asp in 4%. In P3, the small polar amino acids Ser and Thr, which both contain a -OH functional group, were found in 24% of the sequences and Ala and Gly with a small or no side chain were found in 26%. Finally, in the P′1 position, Ala was observed in almost half of the sequences (Figure 5). On the basis of this analysis, a second consensus sequence emerged [i.e., (D/E)-(R/K)-G-(E/D)-(A/G/T/S)-G-P-A or (acidic AA)-(basic AA)-G-(acidic AA)-(small/polar OH AA)-G-P-A)]. This consensus sequence is found in 15 of the 101 peptide sequences within the cleavage map (Figure 4).

To determine whether these consensus sequence motifs represented FAP-preferred cleavage sites or instead were merely observed due to a relative abundance of these particular sequences within the overall gelatin amino acid sequence, we evaluated the frequency of occurrence of these sites within the gelatin protein (Table 1). Overall there were 66 FAP cleavage sites within the 100 kDa recombinant gelatin. A total of 116 G-P sites are found within the protein, and 40 (34%) of these were cleaved by FAP, Table 1. To emphasize the importance of the Ala in the P′1 position, 28 sites with the tripeptide G-P-A exist in the gelatin sequence (24% of total G-P-containing sites). However, when present, 71% of these sites were cleaved by FAP. In addition, on the basis of the cleavage site analysis, we evaluated the frequency

Table 2: Enzyme Kinetics of FAP Substrates Generated from Cleavage Sites within 100 kDa Gelatin

no.	substrate sequence	K_m (μM)	V_m (mol/s)	k_{cat} (s^{-1})	k_{cat}/K_m ($M^{-1}\,s^{-1}$)	normalized ion current rank
1	Mca-ASGPAGPA-Dnp	36.1 ± 2.7	2.26E−12 ± 8.14E−14	0.196 ± 0.007	5441 ± 478	2
2	Mca-EPGPPGPA-Dnp	26.9 ± 0.7	1.32E−12 ± 9.53E−14	0.115 ± 0.006	4270 ± 90	5
3	Mca-DRGETGPA-Dnp	21.0 ± 2.2	8.50E−13 ± 1.89E−14	0.081 ± 0.002	3851 ± 366	3, 4, 7
4	Mca-VGPAGK-Dnp	52.0 ± 4.4	1.09E−12 ± 4.41E−14	0.095 ± 0.004	1822 ± 100	13, 21
5	Mca-DKGESGPA-Dnp	46.0 ± 3.5	7.69E−13 ± 2.11E−14	0.067 ± 0.001	1453 ± 99	20, 24
6	Mca-APGSKGDA-Dnp	51.0 ± 11.8	1.68E−13 ± 1.95E−13	0.015 ± 0.017	286 ± 391	51

Table 3: Enzyme Kinetics of FAP Substrates Derived from the Consensus Sequence DRGETGPA

no.	substrate sequence	K_m (μM)	V_m (mol/s)	k_{cat} (s^{-1})	k_{cat}/K_m ($M^{-1}\,s^{-1}$)
7	Mca-DRGETGP-Dnp	23.8 ± 6.8	3.49E−14 ± 8.02E−15	0.003 ± 0.001	127 ± 31.9
8	Mca-DRGETGPA-Dnp	21.0 ± 2.2	8.50E−13 ± 1.89E−14	0.081 ± 0.002	3851 ± 366
9	Mca-ERGETGPA-Dnp	56.7 ± 0.7	1.62E−12 ± 5.20E−14	0.141 ± 0.004	2483 ± 58
10	Mca-ERGETGPAG-Dnp	43.0 ± 3.8	1.39E−12 ± 8.41E−14	0.121 ± 0.007	2810 ± 149
11	Mca-ERGETGPAGG -Dnp	37.1 ± 1.1	9.05E−13 ± 2.69E−12	0.079 ± 0.004	2120 ± 35
12	Mca-DSGETGP-Dnp	39.6 ± 29.7	3.88E−14 ± 8.11E−15	0.003 ± 0.001	85 ± 60
13	Mca-DSGETGPA-Dnp	20.2 ± 0.5	6.74E−13 ± 4.65E−14	0.059 ± 0.004	2900 ± 221
14	Mca-ERGETGPSG-Dnp	51.3 ± 1.9	3.08E−12 ± 1.77E−13	0.268 ± 0.015	5218 ± 316

of the consensus sequence (D/E)-(K/R)-(D/E)-G-(A/G/S/T)-G-P, the expanded consensus sequence (A/D/E/P)-(K/R)-(D/E/P)-G-(A/G/S/T/P)-G-P, in which Pro is also included in the analysis and the P6 position only included the basic amino acids K/R, and the expanded consensus sequence (D/E)-(K/R/P)-(D/E/P)-G-(A/G/S/T/P)-G-P, in which the P7 position included only the acidic amino acids D/E and not Pro or Ala. The (D/E)-(K/R)-(D/E)-G-(A/G/S/T)-G-P sequence is cleaved by FAP three out of the four times it appears in the gelatin sequence, Table 1. Overall unique consensus sequences were found in only 13% of the total G-P cleavage sites in gelatin. However, when present, 60% of these sequences were cleaved by FAP, Table 1. The presence of this sequence, however, was not sufficient to produce FAP cleavage in the absence of proline in the P1 amino acid, thus further confirming the importance of proline in this position. Seven such sequences containing (A/D/E/P)-(K/R/P)-(D/E/P)-G-(A/G/S/T/P)-G-(non-proline) were identified in the gelatin sequence, and none of these were cleaved by FAP (Table 1). These results demonstrate that the frequent appearance of the (D/E)-(K/R)-(D/E)-G-(A/G/S/T)-G-P sequence in the cleavage fragments is not due to the frequent occurrence of this motif in the overall gelatin sequence, but is rather due to FAP preference for cleavage after this consensus site.

FAP Hydrolysis of Fluorescence-Quenched Peptides Based on the Gelatin Cleavage Map. While previous studies had already determined that FAP preferred to cleave after the dipeptide GP, the normalized ion current analysis also suggested a strong preference for cleavage after GP as well as a strong preference for cleavage of the peptide with GP in P2−P1 and Ala in P′1. To determine whether this type of cleavage site ranking based on the abundance of each extracted ion in the MS spectra would help predict which sequences represented good FAP substrates, we proceeded to synthesize a series of fluorescently quenched peptide substrates based on the cleavage sequences. For this analysis, we generated peptide substrate from sequences with high (i.e., ASGPAGPA, DRGETGPA), intermediate (i.e., EKGESGP, VGPAGK), and low (i.e., GARGQAG, APGSKGDA) extracted ion currents, Figure 4. Michaelis−Menten kinetic parameters (i.e., K_m, V_{max}, k_{cat}) of FAP hydrolysis of these fluorescence-quenched peptides were determined. k_{cat}/K_m ratios were calculated to rank these peptides as FAP substrates (Table 2).

The Mca-ASGPAGPA-Dnp substrate (**1**) had the highest k_{cat}/K_m ratio (Table 2). This peptide sequence was also based on a cleavage fragment with the second highest extracted ion current. Substrate **2**, based on the fragment with the fifth ranked extracted ion current, had the second highest k_{cat}/K_m ratio. In addition, the Mca-DRGETGPA-Dnp substrate (**3**) had the third highest ratio. This substrate is based on a consensus sequence that is the second most common cleavage site in the map and which is found in cleavage fragments with the third, fourth, and seventh highest extracted ion currents. In contrast, the Mca-APGSKGDA-Dnp substrate (**6**), which was least efficiently cleaved by FAP, was based on the cleavage fragment with the lowest overall extracted ion current (Figure 4). Formal kinetic studies were not performed on a second substrate, Mca-GARGQAG-Dnp, based on the fragment with the 47th ranked extracted ion current, but this substrate demonstrated a low hydrolysis rate compared to rates from an equimolar concentration (i.e., 200 μM) of substrates **1**−**5**. Two other substrates with intermediate K_{cat}/K_m ratios [i.e., Mca-VGPAGK-Dnp (**4**) and Mca-DKGESGPA-Dnp (**5**)] were found in cleavage fragments with intermediate extracted ion currents (Table 2).

In a final set of studies, we synthesized additional fluorescence-quenched peptides to explore the importance of amino acids in the P′ positions on the carboxy terminal side of the cleavage site (Table 3). A comparison of the K_{cat}/K_m ratios of substrate **7** with no P′1 amino acid to **8** and substrate **12** to **13** demonstrated that FAP prefers an amino acid in the P′1 position. Both substrates lacking the P′1 alanine were poorly hydrolyzed by FAP. The addition of a P′2 Gly as in **10** or a P′3 Gly as in substrate **11** did not substantially improve the kinetic ratio. Other comparisons demonstrated a slight preference for Asp in the P7 position as in substrate **8** compared to Glu as in substrate **9**. In the P6 position, substitution of Ser as in substrate **13** for Arg as in substrate **8** resulted in some decrease in the kinetic ratio. Finally, in the P′1 position, while Ser was only observed in 12% of the sequences compared to 47% for Ala, the substitution of Ser in the P′1 position as in substrate **14**

resulted in a substantial increase in the k_{cat}/K_m ratio compared to that of the comparable substrate **10** containing Ala in this position (Table 3). The substitution of Ser in the P′1 position generated a peptide substrate with a k_{cat} that was 2−5 fold higher than that of other active substrates.

DISCUSSION

The overall goal of this study was to develop a method to identify substrates on the basis of FAP's collagenase or gelatinase activity. This knowledge of substrate specificity can be used to elucidate FAP's biological role as well as for development of targeted therapeutic prodrugs. Substrate specificity can be defined by using either by high-throughput methods such as the positional scanning synthetic combinatorial library (*15*) and one-bead one-peptide library (*23*) or phage display (*24*, *25*). However, these methods have the disadvantage of an artificial scaffold which can alter the physiological substrate specificity of a protease. Here we have described an approach to take a known protein substrate for a protease and map its cleavage site using proteomics. In the case of FAP, the problem was more complicated because of the polymeric nature of the collagen I protein coupled with multiple types of post-translational modifications.

A large number of collagenases and gelatinases have been previously reported in the literature. However, for most of them substrate characterization was done using combinatorial libraries or synthetic model substrates (*24*, *26*−*29*). To our knowledge there is only one prior reported study in which the collagen protein was digested with a new type of collagenase and cleavage sites determined by Edman sequencing of specific bands isolated on SDS−PAGE (*30*). However, in this previous study only 10−12 cleavage fragments were obtained. Thus, it was possible to easily separate them by SDS−PAGE (*30*). In contrast, in our study the FAP digest of collagen or gelatin produced more than 100 fragments, which produced a smear on SDS−PAGE, rather than discrete bands. This result suggested that FAP cleaved collagen at many sites, thus making traditional Edman sequencing impractical. On this basis, we proceeded to develop the LC/MS/MS-based approach to map these FAP cleavage sites.

Denatured human collagen I was digested with FAP, and small size fragments (<3 kDa) were purified for MALDI-TOF analysis. Previously, MADLI-TOF has been used to identify proteins by analysis of tryptic digests (*31*). Mass spectra revealed that FAP was cleaving collagen I at specific sites. However, sites could not be identified by MALDI-TOF because each mass peak frequently matched more than 10 individual sequences within the collagen I protein. An attempt was also made to perform an LC/tandem MS/MS analysis on these fragments. However, the mass spectroscopic data could not be solved because of collagen's several post-translational modifications (PTMs) that include proline hydroxylation, glycosylation, and cross-linking. Many of these PTMs have not been characterized within collagen I, and therefore, we determined that nonrecombinant, purified human collagen I could not be easily used for such an analysis.

To solve these problems, we identified a source of recombinant gelatin derived from human collagen I that had no PTMs and which could be used for FAP cleavage mapping (*22*). After validating the LC/MS based method using the 8.5 kDa gelatin fragment, we proceeded to generate the map of all FAP cleavage sites within full-length 100 kDa human collagen I derived gelatin. Sequence analysis of the 51 peptide fragments from this digest confirmed earlier reported studies documenting that FAP has a preference for the dipeptide GP in the P2−P1 position. However, these earlier studies, based on a positional scanning method, reported a strict requirement for G-P for FAP hydrolysis. In contrast to these results, we documented that, while FAP prefers cleavage after the G-P dipeptide, FAP can also cleave peptides containing other amino acids in the P1 position (i.e., Ala, Arg, Asp, Gly, Glu, Lys, Ser, and Val).

One disadvantage of the positional scanning synthetic approach is that it often does not yield much specific sequence information beyond the P2−P3 position of the peptide. For the case of FAP, Edosada et al., using positional scanning, documented a preference for Ser or Ala in the P3 position (*32*). This finding also emerged from our cleavage map analysis, in which Ser/Thr was observed in 24% of the sequences in P3 and Ala was observed in 11%. In the study of Edosada et al., no preference could be observed in P4 (*32*). Using a map of a known protein substrate, in this case, allowed us to obtain additional sequence information beyond P3, with sequence preferences emerging for P4, P6, and P7 from the analysis of the cleavage map.

An added advantage of this LC/MS/MS sequencing approach is that it allowed us to quantify the abundance of each identified peptide by comparing the extracted ion current for each of the observed peptide parent ions from the MS spectra. The contribution of each parent ion to the total ion current could then be extracted and integrated over the peptide elution peak. This approach allowed us to rank the peptide fragments on the basis of the extracted ion current. Traditional Edman sequencing does not provide the potential for such fragment stratification. While it was already known before this study that FAP preferred cleavage after proline, this information could also have been learned initially from analysis of the cleavage fragments ranked by the extracted ion current.

Since the abundance of each individual fragment depends on cleavage from two sites, the extracted ion current for each fragment represents an "average" based on the efficiency of FAP cleavage at both sites. Therefore, initially, we thought the ranking would provide no additional information beyond the prediction of a preferred amino acid in the P1 position. To evaluate the utility of this ranking based on ion abundance, we synthesized seven fluorescently quenched peptide substrates based on peptide sequences from fragments with high, intermediate, and low extracted ion currents and determined FAP hydrolysis kinetics for each. The extracted ion current rankings corresponded well with the k_{cat}/K_m ratios of these peptide substrates, with the highest ranked having the highest ratio, etc. Although based on a limited sample of peptide substrates, these results suggest that this method of ranking cleavage sites could be applied to the analysis of cleavage maps of other proteases with unknown substrate specificity to help identify the best substrates for further synthesis and evaluation.

In conclusion, we have used an LC/MS/MS-based method to generate a map of all FAP cleavage sites within recom-

binant human collagen I derived gelatin. From this map, we identified potential consensus peptide sequences that could be used to generate FAP-selective peptide−cytotoxin prodrugs. These FAP-activated prodrugs would selectively target FAP-producing myofibroblasts within the stroma of epithelial tumors and, therefore, would represent a potential "pan-tumor" therapeutic agent. Further studies are under way in our laboratory to assess the efficiency and specificity of these consensus peptides for FAP hydrolysis compared to those of other proteases. In addition, we are further evaluating the role of proline hydroxylation of some of these substrates to determine whether such modification enhances FAP hydrolysis.

ACKNOWLEDGMENT

We acknowledge the Mass Spectrometry/Proteomics Facility at the Johns Hopkins University School of Medicine (www.hopkinsmedicine.org/msf/) for assistance with MALDI-TOF analyses and Dr. John Isaacs for helpful comments related to preparation of the manuscript.

REFERENCES

1. Dvorak, H. F. (1986) Tumors: wounds that do not heal. Similarities between tumor stroma generation and wound healing, *N. Engl. J. Med. 315*, 1650−1659.
2. Liotta, L. A., Steeg, P. S., and Stetler-Stevenson, W. G. (1991) Cancer metastasis and angiogenesis: an imbalance of positive and negative regulation, *Cell 64*, 327−336.
3. Basset, P., Bellocq, J. P., Wolf, C., Stoll, I., Hutin, P., Limacher, J. M., Podhajcer, O. L., Chenard, M. P., Rio, M. C., and Chambon, P. (1990) A novel metalloproteinase gene specifically expressed in stromal cells of breast carcinomas, *Nature 348*, 699−704.
4. Brown, L. F., Guidi, A. J., Schnitt, S. J., Van De Water, L., Iruela-Arispe, M. L., Yeo, T. K., Tognazzi, K., and Dvorak, H. F. (1999) Vascular stroma formation in carcinoma in situ, invasive carcinoma, and metastatic carcinoma of the breast, *Clin. Cancer Res. 5*, 1041−1056.
5. Haslam, S. Z., and Woodward, T. L. (2003) Host microenvironment in breast cancer development: epithelial-cell-stromal-cell interactions and steroid hormone action in normal and cancerous mammary gland, *Breast Cancer Res. 5*, 208−215.
6. Iozzo, R. V. (1995) Tumor stroma as a regulator of neoplastic behavior. Agonistic and antagonistic elements embedded in the same connective tissue, *Lab. Invest. 73*, 157−160.
7. Garin-Chesa, P., Old, L. J., and Rettig, W. J. (1990) Cell surface glycoprotein of reactive stromal fibroblasts as a potential antibody target in human epithelial cancers, *Proc. Natl. Acad. Sci. U.S.A. 87*, 7235−7239.
8. Aoyama, A., and Chen, W. T. (1990) A 170-kDa membrane-bound protease is associated with the expression of invasiveness by human malignant melanoma cells, *Proc. Natl. Acad. Sci. U.S.A. 87*, 8296−8300
9. Rettig, W. J., Garin-Chesa, P., Beresford, H. R., Oettgen, H. F., Melamed, M. R., and Old, L. J. (1988) Cell-surface glycoproteins of human sarcomas: differential expression in normal and malignant tissues and cultured cells, *Proc. Natl. Acad. Sci. U.S.A. 85*, 3110−3114.
10. Scanlan, M. J., Raj, B. K., Calvo, B., Garin-Chesa, P., Sanz-Moncasi, M. P., Healey, J. H., Old, L. J., and Rettig, W. J. (1994) Molecular cloning of fibroblast activation protein alpha, a member of the serine protease family selectively expressed in stromal fibroblasts of epithelial cancers, *Proc. Natl. Acad. Sci. U.S.A. 91*, 5657−61.
11. Kelly, T. (2005) Fibroblast activation protein-alpha and dipeptidyl peptidase IV (CD26): cell-surface proteases that activate cell signaling and are potential targets for cancer therapy, *Drug Resist. Updates 8*, 51−8.
12. Park, J. E., Lenter, M. C., Zimmermann, R. N., Garin-Chesa, P., Old, L. J., and Rettig, W. J. (1999) Fibroblast activation protein, a dual specificity serine protease expressed in reactive human tumor stromal fibroblasts, *J. Biol. Chem. 274*, 36505−36512.
13. Denmeade, S. R., Nagy, A., Gao, J., Lilja, H., Schally, A., and Isaacs, J. (1998) Enzymatic activation of a doxorubicin-peptide prodrug by prostate-specific antigen, *Cancer Res. 58*, 2537−2540.
14. Denmeade, S. R., Jakobsen, C. M., Janssen, S., Khan, S. R., Garrett, E. S., Lilja, H., Christensen, S. B., and Isaacs, J. T. (2003) Prostate-specific antigen-activated thapsigargin prodrug as targeted therapy for prostate cancer, *J. Natl. Cancer Inst. 95*, 990−1000.
15. Janssen, S., Jakobsen, C. M., Rosen, D. M., Ricklis, R. M., Reineke, U., Christensen, S. B., Lilja, H., and Denmeade, S. R. (2004) Screening a combinatorial peptide library to develop a human glandular kallikrein 2-activated prodrug as targeted therapy for prostate cancer, *Mol. Cancer Ther. 3*, 1439−50.
16. Janssen, S., Rosen, D. M., Ricklis, R. M., Dionne, C. A., Lilja, H., Christensen, S. B., Isaacs, J. T., and Denmeade, S. R. (2006) Pharmacokinetics, biodistribution, and antitumor efficacy of a human glandular kallikrein 2 (hK2)-activated thapsigargin prodrug, *Prostate 66*, 358−68.
17. Mhaka, A., Gady, A. M., Rosen, D. M., Lo, K. M., Gillies, S. D., and Denmeade, S. R. (2004) Use of methotrexate-based peptide substrates to characterize the substrate specificity of prostate-specific membrane antigen (PSMA), *Cancer Biol. Ther. 3*, 551−8.
18. Sun, S., Albright, C. F., Fish, B. H., George, H. J., Selling, B. H., Hollis, G. F., and Wynn, R. (2002) Expression, purification, and kinetic characterization of full-length human fibroblast activation protein, *Protein Expr. Purif. 24*, 274−281.
19. Piñeiro-Sánchez, M. L., Goldstein, L. A., Dodt, J., Howard, L., Yeh, Y., Tran, H., Argraves, W. S., and Chen, W. T. (1997) Identification of the 170-kDa melanoma membrane-bound gelatinase (seprase) as a serine integral membrane protease, *J. Biol. Chem. 272*, 7595−601.
20. Christiansen, V. J., Jackson, K. W., Lee, K. N., and McKee, P. A. (2007) Effect of fibroblast activation protein and alpha2-antiplasmin cleaving enzyme on collagen types I, III, and IV, *Arch. Biochem. Biophys. 457*, 177−86.
21. Bulleid, N. J., John, D. C., and Kadler, K. E. (2000) Recombinant expression systems for the production of collagen, *Biochem. Soc. Trans. 28*, 350−353.
22. Olsen, D., Jiang, J., Chang, R., Duffy, R., Sakaguchi, M., Leigh, S., Lundgard, R., Ju, J., Buschman, F., Truong-Le, V., Pham, B., and Polarek, J. W. (2005) Expression and characterization of a low molecular weight recombinant human gelatin: development of a substitute for animal-derived gelatin with superior features, *Protein Expr. Purif. 40*, 346−357.
23. Backes, B. J., Harris, J. L., Leonetti, F., Craik, C. S., and Ellman, J. A. (2000) Synthesis of positional-scanning libraries of fluorogenic peptide substrates to define the extended substrate specificity of plasmin and thrombin, *Nat. Biotechnol. 18*, 187−193.
24. Deng, S. J., Bickett, D. M., Mitchell, J. L., Lambert, M. H., Blackburn, R. K., Carter, H. L., Neugebauer, J., Pahel, G., Weiner, M. P., and Moss, M. L. (2000) Substrate specificity of human collagenase 3 assessed using a phage-displayed peptide library, *J. Biol. Chem. 275*, 31422−31427.
25. Matthews, D. J., and Wells, J. A. (1993) Substrate phage: selection of protease substrates by monovalent phage display, *Science 260*, 1113−1117.
26. Knauper, V., Lopez-Otin, C., Smith, B., Knight, G., and Murphy, G. (1996) Biochemical characterization of human collagenase-3, *J. Biol. Chem. 271*, 1544−1550.
27. McGeehan, G. M., Bickett, D. M., Green, M., Kassel, D., Wiseman, J. S., and Berman, J. (1994) Characterization of the peptide substrate specificities of interstitial collagenase and 92-kDa gelatinase. Implications for substrate optimization, *J. Biol. Chem. 269*, 32814−32820.
28. Matsushita, O., Yoshihara, K., Katayama, S., Minami, J., and Okabe, A. (1994) Purification and characterization of Clostridium perfringens 120-kilodalton collagenase and nucleotide sequence of the corresponding gene, *J. Bacteriol. 176*, 149−156.
29. Hori, H., and Nagai, Y. (1979) Purification of tadpole collagenase and characterization using collagen and synthetic substrates, *Biochim. Biophys. Acta 566*, 211−221.

30. Tsu, C. A., Perona, J. J., Schellenberger, V., Turck, C. W., and Craik, C. S. (1994) The substrate specificity of Uca pugilator collagenolytic serine protease 1 correlates with the bovine type I collagen cleavage sites, *J. Biol. Chem. 269*, 19565−19572.
31. Patterson, S. D., and Aebersold, R. (1995) Mass spectrometric approaches for the identification of gel-separated proteins, *Electrophoresis 16*, 1791−1814.
32. Edosada, C. Y., Quan, C., Wiesmann, C., Tran, T., Sutherlin, D., Reynolds, M., Elliott, J. M., Raab, H., Fairbrother, W., and Wolf, B. B. (2006) Selective inhibition of fibroblast activation protein protease based on dipeptide substrate specificity, *J. Biol. Chem. 281*, 7437−7444.

BI701921B

Targeting the cancer stroma with a fibroblast activation protein-activated promelittin protoxin

Aaron M. LeBeau,[1] W. Nathaniel Brennen,[1] Saurabh Aggarwal,[2] and Samuel R. Denmeade[1,2,3]

Departments of [1]Pharmacology and Molecular Sciences and [2]Chemical and Biomolecular Engineering, and [3]The Sidney Kimmel Comprehensive Cancer Center at Johns Hopkins The Johns Hopkins University, Baltimore Maryland

Abstract

Fibroblast-Activation Protein-α (FAP) is a membrane-bound serine protease that is expressed on the surface of reactive stromal fibroblasts present within the majority of human epithelial tumors but is not expressed by normal tissues. FAP is a postprolyl peptidase that differs from other dipeptidyl prolyl peptidases such as diprolylpeptidase 4 in that it also has gelatinase and collagenase endopeptidase activity. Therefore, FAP represents a potential pan-tumor target whose enzymatic activity can be exploited for the intratumoral activation of prodrugs and protoxins. To evaluate FAP as a tumor-specific target, putative FAP-selective peptide protoxins were constructed through modification of the prodomain of melittin, a 26 amino acid amphipathic cytolytic peptide that is the main toxic component in the venom of the common European honeybee *Apis milefera*. Melittin is synthesized as promelittin, containing a 22 amino acid NH_2-terminal prodomain rich in the amino acids proline and alanine. In this study, peptides containing truncated melittin prodomain sequences were tested on erythrocytes to determine the optimal prodomain length for inhibiting cytolytic activity. Once optimized, modified promelittin peptides were generated in which previously identified FAP substrate sequences were introduced into the prodomain. Peptide protoxins were identified that were efficiently activated by FAP and selectively toxic to FAP-expressing cell lines with an IC_{50} value in the low micromolar range that is similar to melittin. Intratumoral injection of an FAP-activated protoxin produced significant lysis and growth inhibition of human breast and prostate cancer xenografts with minimal toxicity to the host animal. [Mol Cancer Ther 2009;8(5):1378–86]

Introduction

The growth of an epithelial neoplasm requires the formation of a supporting tumor stroma to supply nutrients and growth factors for tumor cell survival and continued growth. This invasive growth is associated with characteristic changes in the supporting stroma that include the induction of tumor blood vessel formation; the recruitment of reactive stromal fibroblasts, lymphocytes, and macrophages; the release of peptide-signaling molecules and proteases; and the production of an altered extracellular matrix (1–5). The tumor stroma compartment represents a major component of the mass of most carcinomas, with 20% to 50% commonly seen in breast, lung, and colorectal cancers and reaching >90% in carcinomas that have desmoplastic reactions (5, 6).

Reactive tumor stromal fibroblasts differ from fibroblasts of normal adult tissues with regard to morphology, gene expression profiles, and production of important biological mediators such as growth factors and proteases (1, 7, 8). A highly consistent trait of tumor stromal fibroblasts is the induction of the membrane-bound serine protease fibroblast-activation protein-α (FAP). FAP was originally identified as an inducible antigen expressed on reactive stroma and given the name Fibroblast Activation Protein. FAP was independently identified by a second group as a gelatinase expressed by aggressive melanoma cell lines and was given the name "seprase" for surface expressed protease (9). Subsequent cloning of FAP and seprase revealed that they are the same cell-surface serine protease (10).

FAP was originally reported to be a cell-surface antigen recognized by the F19 monoclonal antibody on human astrocytes and sarcoma cell lines *in vitro* (11). In one series using human tissues, FAP was detected in the stroma of over 90% of malignant breast, colorectal, skin, and pancreatic tumors (7, 11). In a small study, FAP was detected in the stroma of 7of 7 prostate cancers (12). FAP is also expressed by a subset of soft tissue and bone sarcomas (7). FAP-positive fibroblasts also accompany newly formed tumor blood vessels (10). In nonmalignant tissue, FAP is expressed by reactive fibroblasts in wound healing, rheumatoid arthritis, liver cirrhosis, and in some fetal mesenchymal tissues (7). Cheng et al. (13) also showed that, such as human FAP, mouse FAP is expressed by reactive fibroblasts within human cancer xenografts. In contrast, most normal adult tissues show no detectable FAP protein expression (7). In a recent study, Ghilardi et al. (14) used real-time PCR to quantify gene expression from laser

Received 9/17/08; revised 2/11/09; accepted 2/19/09; published OnlineFirst 5/5/09.

Grant support: NIH grant 5RO1CA124764 to SRD and a DOD prostate cancer predoctoral mentorship grant W81XWH-07 (W.N. Brennen).

The costs of publication of this article were defrayed in part by the payment of page charges. This article must therefore be hereby marked *advertisement* in accordance with 18 U.S.C. Section 1734 solely to indicate this fact.

Requests for reprints: Samuel R. Denmeade, Department of Oncology, The Johns Hopkins University School of Medicine, Cancer Research Building I, Rm 1M43, 1650 Orleans Street, Baltimore, MD 21231. Phone: 410-955-8875; Fax: 410-614-8397. E-mail: denmesa@jhmi.edu

doi:10.1158/1535-7163.MCT-08-1170

capture dissected tumor endothelium and found a significant increase in FAP expression compared with normal endothelium. This suggests that FAP expression may also be induced in both reactive tumor stroma and endothelium.

FAP is a member of the enzyme class known as postprolyl peptidases that are uniquely capable of cleaving the Pro-Xxx amino acid bond (15). This group of proteases includes the well-characterized dipeptidyl peptidase 4 (DPP4) as well as DPP2, DPP6, DPP7, DPP8, DPP9, prolyl carboxypeptidase, and prolyl endopeptidase. The substrate preferences for many of these prolyl peptidases are not entirely known but, such as DPP4, they all have dipeptidase activity. Like DPP4, FAP is a type II integral membrane protein able to cleave peptides containing proline as the penultimate amino acid. FAP differs from DPP4 in that it also has gelatinase and collagenase activity (16). This additional gelatinase/collagenase activity may be unique to FAP among the family of prolyl proteases.

The selective tumor expression and unique enzymatic activity of FAP make it a potentially attractive therapeutic target. Recently, our laboratory mapped all of the FAP cleavage sites in recombinant human gelatin and identified a series of peptide substrates that are efficiently cleaved by FAP (17). These peptide substrates can be coupled to cytotoxic small molecules to make FAP-activated prodrugs. Alternatively, the peptides could be incorporated into the activation domain of cytolytic proteins and peptides to produce FAP-activated protoxins. In this regard, we have generated an FAP-activated peptide toxin by incorporating an FAP-selective peptide sequence into the prodomain of the cytolytic peptide melittin.

Melittin, a 26 amino acid amphipathic peptide, is the main toxic component in the venom of the common European honeybee *Apis milefera* (18). The ability of melittin to induce the lysis of prokaryotic and eukaryotic cells has been well-documented (19–21). The exact mechanism by which melittin disrupts both natural and synthetic phospholipid bilayers is still largely unknown. In an aqueous milieu, melittin has a net + 6 charge and exists as a random coiled monomer. It has been suggested that melittin can produce its toxic effects either by forming a transmembrane pore structure made up of melittin aggregates or by binding to the membrane surface and acting in a detergent-like manner leading to an increase in membrane permeability (18, 21).

In the honeybee, melittin is secreted into the venom glands as promelittin possessing an NH_2-terminal prodomain made up of 22 amino acids. The prodomain is highly negatively charged containing nine acidic amino acid residues (22). The presence of the prodomain confers an overall negative charge to the molecule and decreases the ability of melittin to interact with the surface of the cell membrane. In the prodomain amino acid sequence, every second amino acid is either proline or alanine. Promelittin activation *in vivo* is the result of the stepwise cleavage of the prodomain into 11 dipeptide fragments by a DPP4-like protease present in honeybee venom gland extracts (22). By acetylating the promelittin peptide or adding an extra amino acid residue at the NH_2 terminus, the stepwise activation of promelittin by DPP4 dipeptidase activity is prevented. This observation suggested that the promelittin prodomain could be readily reengineered to produce a prodomain that can be removed by a non–DPP4-like endopeptidase such as FAP. In this study, we report studies done to determine the minimal prodomain length required to inactivate the cytolytic activity of melittin. Subsequently, we substituted putative FAP peptide substrates into this truncated prodomain to identify an FAP-melittin peptide that is selectively toxic to FAP-producing cells. Finally, we evaluated the antitumor effect of an FAP-melittin protoxin after intratumoral injection of peptide into human prostate and breast cancer xenografts.

Materials and Methods

All reagents for Fmoc solid-phase peptide synthesis were purchased from Anaspec. Unless stated otherwise, all other reagents were purchased from Sigma. His-tagged FAP lacking the transmembrane domain was produced and purified in our laboratory as previously described (17). FAP activity was confirmed through activation of the dipeptide substrate Ala-Pro-AFC.

Cell Lines

The human prostate cancer cell line LNCaP and the human breast cancer cell line MCF-7 were purchased from American Type Culture Collection. LNCaP was maintained in RPMI 1640 and MCF-7 in DMEM media supplemented with 10% serum, 1% pen/strep, and 2 mmol/L L-glutamine (Invitrogen) in a 37°C incubator with 5% CO_2 and 98% humidity as previously described (23).

Generation of FAP-Transfected Cells

The full-length human FAP cDNA was generated as previously described (17) and cloned into the multiple cloning site of a pIRESneo3 vector (Clontech). Neomycin-selected colonies were obtained and evaluated for FAP expression through fluorescence-activated cell sorting analysis using supernatant from an anti-FAP F19 monoclonal antibody producing hybridoma line obtained from American Type Culture Collection as the primary antibody. Colonies expressing the highest levels of FAP were expanded and maintained under neomycin selection for use in *in vitro* studies.

Peptide Synthesis

Promelittin peptides were synthesized on Fmoc-Gln(Trt) Rink amide 4-methyl benzhydrylamine resin and were elongated using standard Fmoc solid-phase peptide conditions on an AAPPTEC Apex 396 peptide synthesizer as previously described (24). The prodomain for each peptide was of variable length, but the mature melittin peptide sequence, NH_2-GIGAVLKVLTTGLPALISWIKRKRQQ-NH_2, was the same for each peptide. The cleavage and deprotection of the peptides from the resin were carried out using a cleavage cocktail of trifluoroacetic acid/thioanisole/water/phenol/EDT (82.5:5:5:5:2.5, v/v) for 4 h. The peptides were precipitated from the cleavage cocktail using cold ether and dissolved in water for reversed-phase high-performance liquid chromatography purification. Reversed-phase high-performance liquid chromatography purification was

Table 1. Prodomain amino acid sequence of promelittin peptides

Toxin		HD_{50} (μmol/L)	Net charge
PM11	APEPEPAPEPEAEADAEADPEA	>100	−3
PM11a	PEPEPAPEPEAEADAEADPEA	>100	−3
PM10	EPEPAPEPEAEADAEADPEA	>100	−3
PM10a	PEPAPEPEAEADAEADPEA	>100	−2
PM9	EPAPEPEAEADAEADPEA	95.5 ± 3.4	−2
PM9a	PAPEPEAEADAEADPEA	73.0 ± 4.7	−1
PM8	APEPEAEADAEADPEA	64.0 ± 4.2	−1
PM8a	PEPEAEADAEADPEA	59.3 ± 2.7	−1
PM7	EPEAEADAEADPEA	66.6 ± 2.9	−1
PM7a	PEAEADAEADPEA	52.0 ± 2.3	0
PM6	EAEADAEADPEA	55.9 ± 3.5	0
PM6a	AEADAEADPEA	48.4 ± 1.9	1
PM5	EADAEADPEA	37.6 ± 2.5	1
PM5a	ADAEADPEA	29.2 ± 1.8	2
PM4	DAEADPEA	22.3 ± 1.1	2
PM4a	AEADPEA	11.8 ± 0.6	3
PM3	EADPEA	8.6 ± 0.3	3
PM3a	ADPEA	6.2 ± 0.2	4
PM2	DPEA	4.7 ± 0.3	4
PM2a	PEA	1.8 ± 0.1	5
PM1	EA	1.7 ± 0.1	5
PM1a	A	1.5 ± 0.1	6
PM0		1.3 ± 0.1	6

NOTE: HD_{50}, concentration required to lyse 50% of RBC in a 2% RBC solution. Charge, net charge on the full length peptide.

done on a Waters Δ 600 semiprep system using a Phenomenex Luna 10u C_{18} 250 × 10 mm semiprep column. The high-performance liquid chromatography gradient profile was linear starting at 100% solvent A (0.1% trifluoroacetic acid in H_2O) and changing to 100% solvent B (0.1% trifluoroacetic acid in acetonitrile) over 25 min with a flow rate of 8 mL/min. Fractions of the desired purity (>95% as determined using an analytic reversed-phase high-performance liquid chromatography) were pooled and lyophilized. The purified promelittin peptides were mass analyzed on an Applied Biosystems Voyager DE-STR MALDI-TOF mass spectrometer at the Johns Hopkins School of Medicine Mass Spectrometry and Proteomics Facility using a matrix of 10 mg/mL 2,5-dihydroxy benzoic acid in 50% ethanol/water. The mass spectrometer was calibrated using the ProteoMass Peptide MALDI Calbration kit (Sigma). All spectra were acquired in the positive ion mode.

Hemolysis Assays

Hemolysis assays were done as previously described (23). Briefly, peptides were dissolved in DMSO and serially titrated by 2-fold dilution using 1× PBS buffer. The peptides were incubated over a range of concentrations with washed human RBC at a concentration of 2% v/v for 1 h at 37°C. The control for zero hemolysis was RBCs suspended in PBS buffer alone, and the 100% hemolysis control consisted of RBCs in the presence of 1% Triton X-100. After incubation with the peptides, the RBCs were pelleted and 50 μL of each sample were transferred in triplicate to a clear flat-bottomed 96-well polystyrene plate. Hemolysis was assessed by measuring the absorbance of the samples at 540 nm with a Molecular Devices Spectra Max Plus automatic plate reader.

Promelittin FAP Digestion

One hundred micrograms of each promelittin peptide were incubated with 2 μg of purified FAP in 200 μL of FAP assay buffer containing 100 mmol/L Tris, 100 mmol/L NaCl (pH 7.8) at 37°C. Aliquots of the digests were taken every hour for 8 h, desalted using P10-C_{18} ZipTips (Millipore), and spotted (0.5 μL) on a MALDI-TOF plate using the 2,5-dihydroxy benzoic acid matrix. Spectra were collected on an Applied Biosystems Voyager DE-STR MALDI-TOF mass spectrometer in positive ion mode.

Cytotoxicity Assays

Assays were done using MCF-7 breast cancer cells transfected with a full-length FAP expression vector. Vector only–transfected MCF-7 cells served as a control. Cells were exposed to peptides over a range of concentrations for 72 h prior and then cell viability was determined using an 3-(4,5-dimethylthiazol-2-yl)-2,5-diphenyltetrazolium bromide cell proliferation assay (Promega) as previously described and according to manufacturer's instructions (23).

In vivo Assays: Tumor Xenograft Studies

Mouse care and treatment was approved by and done in accordance with the guidelines of the Animal Care and Use Committee of the Johns Hopkins University School of Medicine. Cells maintained under standard conditions were detached by treatment with 0.25% trypsin-EDTA solution and washed in HBSS. They were then suspended in a 60% mixture of Matrigel Matrix (BD Biosciences) in HBSS at a concentration of 2.0×10^6 cells per 100 μL of solution. LNCaP cells were then injected into the subcutis overlying the rear flanks of 6-week-old male nude mice (Harlan). MCF-7 cells were injected s.c. into 6-wk-old female nude mice previously implanted s.c. with a slow release estrogen pellet (0.72 mg of 17β-estradiol; Innovative Research of America) in the contralateral flank. Weekly tumor measurements were made with calipers and the tumor volume (in cm^3) was calculated by the formula $0.5236 \times L \times W \times H$. The mice were euthanized by CO_2 overdose, and the tumors were weighed and processed for histochemical analysis as previously described (23). Balb-c mice (Harlan) were used for i.v. toxicity studies as previously described (23).

Statistical Analysis

For the *in vitro* proliferation studies, P values were derived from the Student's t test. All statistical tests were two-sided, and P value of <0.05 was considered to be statistically significant. For the *in vivo* studies, data, presented as mean ± SE, were evaluated using ANOVA analysis. P value of <0.05 was considered statistically significant.

Results

Promelittin Prodomain Truncation

A total of 22 promelittin peptides, representing every possible prodomain length, were synthesized (Table 1). Using the truncated promelittin peptides, we investigated how much of the prodomain was necessary to inhibit the

cytolytic ability of melittin. The goal was to find the minimal length melittin prodomain that could be subsequently modified to produce the minimal length FAP-activated melittin peptide toxin. Whereas PM11 represents the full-length prodomain, peptides PM0-PM10 represent products of the stepwise two amino acid cleavage of promelittin by DPP4. Peptides PM1a-PM11a are non-DPP4 substrates because they do not contain dipeptide units at the NH_2 terminus ending with either proline or alanine. To assess the relative degree of inhibition of the lytic ability of each promelittin peptide toward eukaryotic cells, human erythrocytes were used as a model membrane. The hemolytic dose necessary to lyse 50% of the erythrocytes (i.e., HD_{50}) was determined for each promelittin peptide (Table 1). These studies revealed that the promelittin peptides containing the longest prodomains were the least hemolytic toward human erythrocytes. The full-length promelittin peptide (PM11), PM11a, PM10, and PM10a, all had HD_{50} values above 100 μmol/L. Appreciable hemolysis was not observed until approximately half of the pro-domain had been removed. PM6, with a 12 amino acid prodomain sequence and a net charge of 0, had an HD_{50} of 55.9 μmol/L. As the pro-domain sequence decreased one amino acid at a time and the net negative charge of the peptide increased, the HD_{50} for each peptide steadily decreased (Table 1). PM0 (melittin) was found to have an HD_{50} of 1.3 μmol/L. Likewise, the 7 shortest promelittin peptides were hemolytic with HD_{50} values at or below 10 μmol/L.

Based on these results, the 14 amino acid pro-domain length of PM7, which had an HD_{50} of 66.6 μmol/L, was selected for further studies aimed at developing an FAP-activated toxin. PM7 was found to be ~50-fold less hemolytic than the fully processed melittin. Although longer length prodomains had higher HD_{50} values in the hemolysis assay, the 40 amino acid PM7 was selected because this starting peptide length allowed for the introduction of modifications and additions to the prodomain that would produce peptides that were <50 amino acids

	Prodomain Sequence	Observed Parental Ion (% Relative Intensity)	Observed Cleavage Product (% Relative Intensity)
FAP1	EP|EAEADAEAGP|EA -mel (3986.75 / 3046.89)	4214.71 (20)	3968.75 (30), 3046.89 (100)
FAP2	EPEAEADAEAGP|A -mel (2918.32)	4084.66 (0)	2918.32 (100)
FAP3	EPEAEADAEADPEAGP|A -mel (2918.48)	4497.73 (100)	2918.48 (70)
FAP4	EPEAEADAEADPEASGEAGP|A -mel (2918.93)	4841.82 (100)	2918.93 (30)
FAP5	EPEAEADAEADPEAPGPPGP|-mel (2846.13)	4774.14 (100)	2846.13 (15)

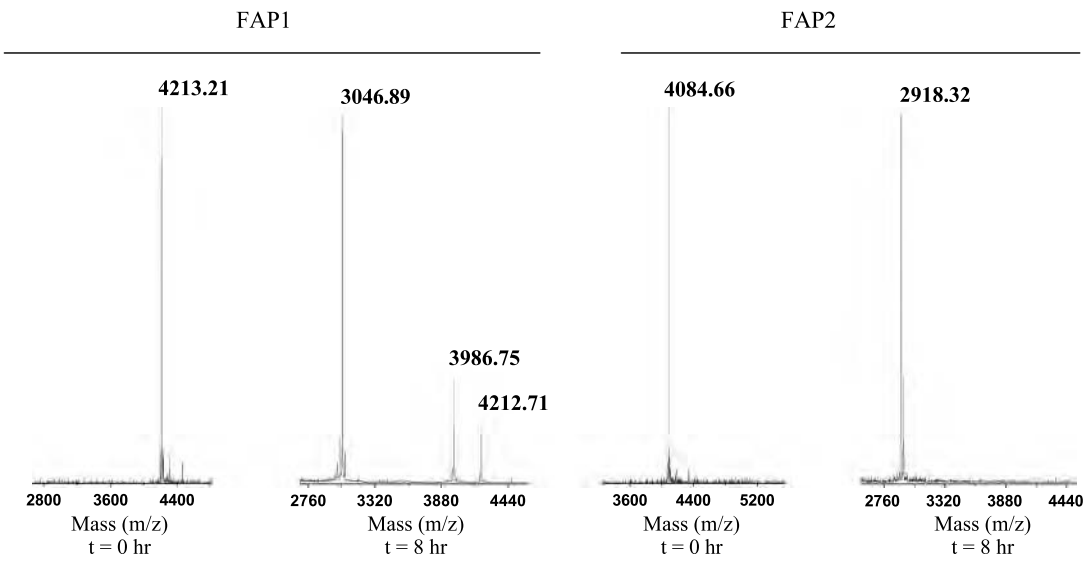

Figure 1. FAP cleavage of the modified promelittin peptides. The prodomain sequence of modified protoxins (*FAP 1-5*) with cleavage site and mass of cleavage fragment delineated. MALDI-TOF analysis was used to evaluate the extent of cleavage. The relative intensity of each mass fragment is based on a comparison of the relative peak height for each individual trace, with the largest peak for each experiment arbitrarily set to 100. *Bottom,* representative MALDI trace for FAP1 and FAP2 (100 μg) at time 0 and 8 h after exposure to active FAP (2 μg total).

in length. Peptides longer than 50 amino acids were technically difficult to synthesize and this precluded the use of longer length promelittins (e.g., PM11) as the starting sequence.

Generation of an FAP-Cleavable Promelittin Protoxins

Previous studies in our laboratory and others have documented that the most preferred FAP-cleavable peptide sequences contain Pro in the P1 position and Gly in the P2 position with a suggestion that Ala in the P′1 position is also favored (17, 25). Based on our previous studies characterizing FAP cleavage substrates from a map of cleavage sites within human gelatin, five candidate protoxins were synthesized using the prodomain of PM7 (i.e., FAP1-5; Fig. 1A; ref. 16). In FAP1, the Asp-4 of the PM7 prodomain was changed to a Gly to reproduce the Gly-Pro preference in the P1 and P2 positions ascribed to FAP (17). Because the effect on the ability of FAP to hydrolyze a peptide containing an acidic Glu residue in the P1 position was not known, FAP2 was designed such that the prodomain sequence was kept the same as that for FAP1 with the exception that Glu-2 of the prodomain of FAP1 was removed to create the FAP preferred P2-P1-P′1 sequence of Gly-Pro-Ala. For FAP3, the P2-P1-P′1 sequence of Gly-Pro-Ala was inserted between the NH_2 terminus of melittin and the full-length native PM7 prodomain sequence. FAP4 had a seven amino acid FAP cleavable peptide substrate (SGEAGPA) inserted between the NH_2 terminus and the PM7 prodomain, whereas FAP5 had a repetitive $(Pro\text{-}Gly\text{-}Pro)_2$ motif inserted between the NH_2 terminus of melittin and the prodomain of PM7. FAP4 and FAP5 were the two largest peptides synthesized, 46 and 47 amino acids, respectively. FAP2 was the shortest, consisting of only 39 amino acids. The hemolytic activity of these FAP candidate protoxins was assayed and all were found to have HD_{50} values between 50 and 70 μmol/L (Table 2).

FAP Cleavage Assays

To assess FAP cleavage, the FAP candidate protoxins were assayed *in vitro* with purified recombinant FAP to characterize the extent of FAP-mediated cleavage. The peptides (100 μg) were digested with FAP (2 μg) for a total of 8 hours at 37°C. Every 2 hours, aliquots were taken and the progress of the digest was monitored using matrix-assisted laser desorption/ionization time-of-flight (MALDI-TOF) mass spectrometry (Fig. 1). After 8 hours, the only protoxin that was completely digested by FAP was FAP2 (Fig. 1). The digested FAP2 yielded only 1 cleavage product with a mass of 2,918.32 m/z, corresponding to the hydrolysis of the Gly-Pro↓Ala bond. FAP1, which differed from FAP2 by only one Glu residue, did show some of the desired cleavage product at 3,046.89 m/z (Fig. 1). However, the FAP1 digest was incomplete, leaving uncut starting material and other cleavage by-products. FAP3, FAP4, and FAP5 were cleaved to varying degrees, but none were cleaved as well as FAP2 (Fig. 1). Finally, although mature melittin also contains an internal proline residue, MALDI-TOF analysis showed that it was not cleaved by FAP (data not shown).

FAP Promelittin Protoxins Selectively Kill FAP-Expressing Human Breast Cancer Cell Lines

To evaluate the selectivity of each FAP-activated protoxin for the ability to kill FAP-positive versus FAP-negative cancer cells, we transfected the human breast cancer cell line MCF-7 with either FAP or vector only controls. These cells were then used to assess the effect of each protoxin on growth as assayed by 3-(4,5-dimethylthiazol-2-yl)-2,5-diphenyltetrazolium bromide assay. In this assay, mature melittin showed no selectivity and was able to kill both cell lines at approximately equally low micromolar concentrations (Table 2). Compared with melittin, the modified promelittin peptides were ~30- to 40-fold less toxic against the vector only–transfected FAP-negative MCF-7 cells. In contrast, against the transfected FAP-producing cell line, FAP2 was the most toxic peptide surveyed with an IC_{50} of 5.2 μmol/L. This peptide was also the most selective and was ~7-fold more active against the FAP-positive versus FAP-negative MCF-7 cells. All of the other promelittin peptides had fold differences in cytotoxicity of less than two (Table 2). FAP2 was the only protoxin in this series that showed a significant therapeutic index *in vitro*.

To eliminate the potential for nonspecific cleavage of the FAP2 sequence by DPP4, we subsequently generated a DPP4-"resistant" version of FAP2 by adding an acetylated NH_2-terminal glycine to the FAP2 peptide to generate Ac-FAP6. Ac-FAP6 was cleaved by FAP to the same extent as FAP2 (data not shown) and had the highest HD_{50} (72 μmol/L) of all of the FAP-activated protoxins (Table 2). This acetylated peptide showed increased specificity with an IC_{50} of 47.9 versus 35.1 μmol/L for FAP2 against FAP-negative cells. However, Ac-FAP6 was nearly as potent as FAP2 with an IC_{50} value of 6.1 μmol/L against FAP-positive cells for an overall higher ~8-fold difference in toxicity against FAP-positive and FAP-negative cells.

In vivo Antitumor Activity of FAP Promelittin Protoxins

Before performing *in vivo* efficacy studies, we did toxicity studies *in vivo* with the administration of the protoxins i.v. and intratumorally. Melittin is a nonspecific cytolytic toxin. Therefore, as expected, melittin was highly toxic to mice with an i.v. LD_{100} (i.e., single dose that kills 100% of

Table 2. HD_{50} values and cytotoxicity of FAP Melittin protoxins against FAP-negative and FAP-positive MCF-7 human breast cancer cells

Toxin	HD_{50} (μmol/L)	IC_{50} (μmol/L)		
		FAP neg	FAP pos	Fold diff
FAP1	56.9 ± 3.1	45.6 ± 5.6	26.8 ± 1.1	1.7
FAP2	54.2 ± 2.2	35.1 ± 2.0	5.2 ± 0.4	6.7
FAP3	60.0 ± 3.7	33.1 ± 2.3	18.9 ± 1.7	1.8
FAP4	70.5 ± 5.1	50.1 ± 4.9	28.1 ± 2.2	1.8
FAP5	67.5 ± 3.5	27.6 ± 1.2	18.3 ± 2.0	1.5
Ac-FAP6	72.2 ± 3.6	47.9 ± 2.9	6.1 ± 0.3	7.9
Melittin	1.3 ± 0.1	1.4 ± 0.1	1.3 ± 0.2	1.1

Abbreviations: FAP neg, FAP negtive; FAP pos, FAP positive; fold diff, fold difference.

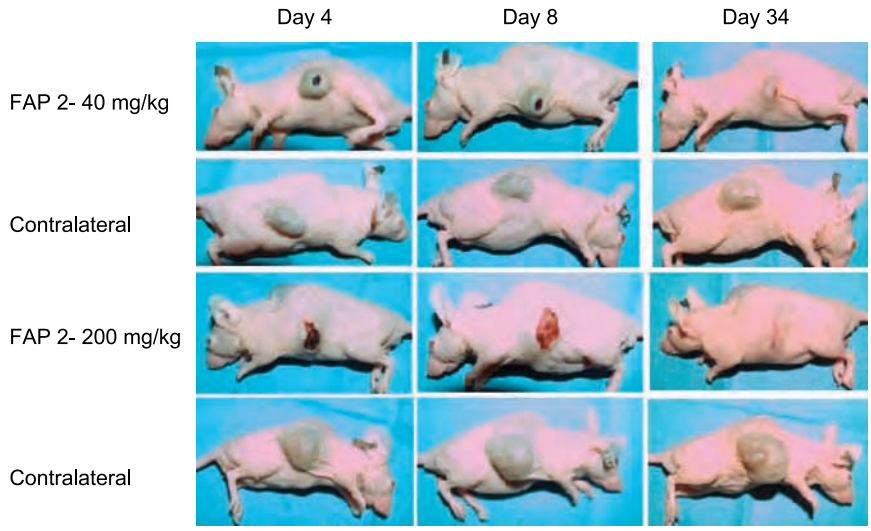

Figure 2. Nude mice bearing LNCaP human prostate cancer xenografts on both flanks were treated with single intratumoral dose of FAP2 at the indicated concentration of FAP2 into the tumor in one flank, with saline injected into the tumor on the contralateral flank. Representative tumor response is shown for 1 animal at each dose level over a 34-d period.

animals) of ~3 mg/kg. i.v., a dose of 1 mg/kg of melittin was the maximally tolerated dose. In contrast, for PM11, FAP2, and Ac-FAP6, a single dose of 40 mg/kg i.v. was tolerated in Balb-c mice, whereas a dose of 100 mg/kg was 100% lethal. The LD_{100} for FAP2 was subsequently found to be lower in tumor-bearing nude mice used in efficacy experiments as a single 40 mg/kg i.v. dose proved lethal to all mice within 1 week posttreatment. For the intratumoral injection studies, the maximum tolerated dose of intratumoral melittin was determined to be 5.7 mg/kg (50 nmoles). In contrast, an intratumoral dose of 40 mg/kg (250 nmoles) of FAP2 was well-tolerated, whereas a dose of 200 mg/kg (1,250 nmoles) was lethal to ~33% of treated animals by 24 hours posttreatment.

A number of studies have documented that FAP expression in mouse stromal cells occurs in a wide variety of human cancer xenografts (13, 26, 27). On the basis of these dose finding studies, an initial cohort of animals (n = 6 per group) bearing LNCaP human prostate cancer xenografts received a single intratumoral injection of either 40 or 200 mg/kg of FAP2 (Fig. 2). Tumors were then imaged serially over a 34-day period. Representative results are shown in Fig. 2. Treated tumors developed a necrotic center and overlying eschar, which eventually healed as the underlying tumor regressed over the observation period. Complete regressions were observed in select animals in the 200 mg/kg group (Fig. 2), but this dose level also resulted in the death of 1 of 3 of the treated animals. No complete regressions were observed in the 40 mg/kg dosing group.

The next experiment was designed to compare the extent of FAP specific versus nonspecific killing after the injection of a series of promelittin toxins into human MCF-7 breast cancer xenografts. This line was selected based on previous studies demonstrating that MCF-7 possesses a moderate amount of stroma and can induce expression of human FAP by human fibroblasts coinoculated with MCF-7 cells (28). For these studies, we compared the single dose efficacy of Ac-FAP6 (FAP-activated, DPP4-resistant, HD_{50} of 72 μmol/L) to PM11 (FAP-resistant, DPP4-activated, HD_{50} of >100 μmol/L). In addition, to generate a toxin that would not be cleaved by FAP or DPP4, we evaluated the effects of acetylating the amino terminus of the PM toxins. In this analysis, we determined that acetylation can lower the HD_{50} compared with the unacetylated protoxin in some instances. From this analysis, we selected the acetylated version of sequence PM9 for *in vivo* studies because this acetylated protoxin had the highest HD_{50} of all of the acetylated peptides tested. Although PM9 had an HD_{50} of 95 μmol/L, Ac-PM9 had an HD_{50} of 76 μmol/L, which was similar to the HD_{50} for Ac-FAP-6. Like Ac-FAP6, Ac-PM 9 is not a substrate for dipeptidyl peptidase IV due to acetylation of the amino terminus and is not cleaved by FAP due to lack of the FAP-preferred Gly-Pro dipeptide in the prodomain. Therefore Ac-PM9 can be considered FAP resistant and DPP4 resistant.

Based on previous toxicity studies, tumor-bearing animals were treated with a single intratumoral dose of 250 nmoles (~40-50 mg/kg) of each of these promelittin toxins. Tumors (n = 3 per group) were then harvested 96 hours postinjection, fixed, and stained. Areas of necrotic tissue were easily seen under low-power magnification with higher power magnification demonstrating areas with pyknotic nuclei in a field of cellular debris (Fig. 3A). Under low-power magnification using image analysis, the total area of the tumor slice was determined as previously described (23). Subsequently, the total area of nonviable tumor tissue was determined and the % area of necrosis was determined from the ratio of these two areas (Fig. 3B). Using this methodology, injection of PM11 resulted in tumors with ~25% necrosis of total tumor cross-sectional area, which was not significantly different than the 16% necrosis seen in control tumors injected with saline (Fig. 3C). Ac-PM9 induced necrosis that was not significantly different than that seen for PM11 (Fig. 3C). In contrast, Ac-FAP6 injection resulted in significant increase in the area of necrosis with ~60% necrosis of tumors at 96 hours postinjection, consistent with

the enhanced distribution and activation of the Ac-FAP6 toxin compared with the non-FAP activated PM11 and Ac-PM9 toxins (Fig. 3C).

In the final experiment, the effect of Ac-FAP6 on the growth rate of tumors after intratumoral injection was compared with the growth rate of saline injected controls (Fig. 4A). Studies were done using an intratumoral treatment approach to evaluate the full extent of activation of the FAP-activated toxin within tumor tissue. After randomization to afford groups of relatively equal starting average tumor size, animals (n = 8 per group) received a single intratumoral injection of either 45 mg/kg (250 nmoles) of Ac-FAP6 or saline and were then followed for an additional 2 weeks posttreatment. No animal deaths or morbidity were observed in either group. In the saline controls, 7 of 8 animals had a doubling of tumor size by day 14 (Fig. 4B). In contrast, only 2 of 8 Ac-FAP6 animals had a doubling of tumor size over this time period (Fig. 4B). Two of the Ac-FAP6–treated animals had a >20% reduction in starting tumor size, with 1 of these animals having a >50% reduction. None of the control animals had any significant reduction in tumor size over the measurement period. A number of the Ac-FAP6 animals had an initial increase in tumor size at day 4 posttreatment followed by a 20% to 65% decrease in size at day 7 posttreatment, possibly due to an initial acute inflammation within the tumor.

Discussion

The goal of these studies was to show the feasibility of targeting the unique proteolytic activity of FAP, a membrane-bound serine protease that is expressed on the surface of reactive fibroblasts present within the stroma of most human tumors. Given its restricted expression in the reactive stroma of potentially >90% of epithelial cancers studied (7), FAP represents an attractive target for tumor-directed therapies. In this study, to provide the initial proof of concept data, we focused on a peptide-based protoxin strategy due to the ease of synthesis and the known ability of FAP to function as an endopeptidase. We showed that the inhibitory prodomain of melittin, a well-characterized toxin produced by the honeybee, could be modified to a form that was no longer hydrolyzed by the native activator protease DPP4 but, instead, was hydrolyzed by FAP.

Although FAP has only recently come to attention as a putative tumor-specific target, considerable effort has already been expended to develop FAP-based therapies. The most obvious therapeutic approach would be to develop inhibitors of FAP function such as monoclonal antibodies (29, 30) or small molecule inhibitors (31–33). These approaches are under preclinical and clinical evaluation. Such strategies would potentially produce a therapeutic benefit if FAP were involved in the promotion of growth within tumors. However, studies to date suggest that the role of FAP in tumor growth may be highly contextual and in some cases, FAP expression may itself be growth inhibitory to tumors (33, 34). Thus, in contrast to these inhibitory strategies, the protoxin strategy described here can be successful regardless of the role of FAP in tumor biology as it takes advantage of the enzymatic activity of FAP to selectively activate a highly potent cytotoxin in the peritumoral fluid. Such activation should not only lead to death of tumor stromal cells but will also generate a significant bystander effect leading to death of tumor cells and endothelial cells within and surrounding the stromal compartment.

Although these studies provide proof of concept, the therapeutic application of this FAP-activated promelittin toxin is limited and would most likely only be useful in settings

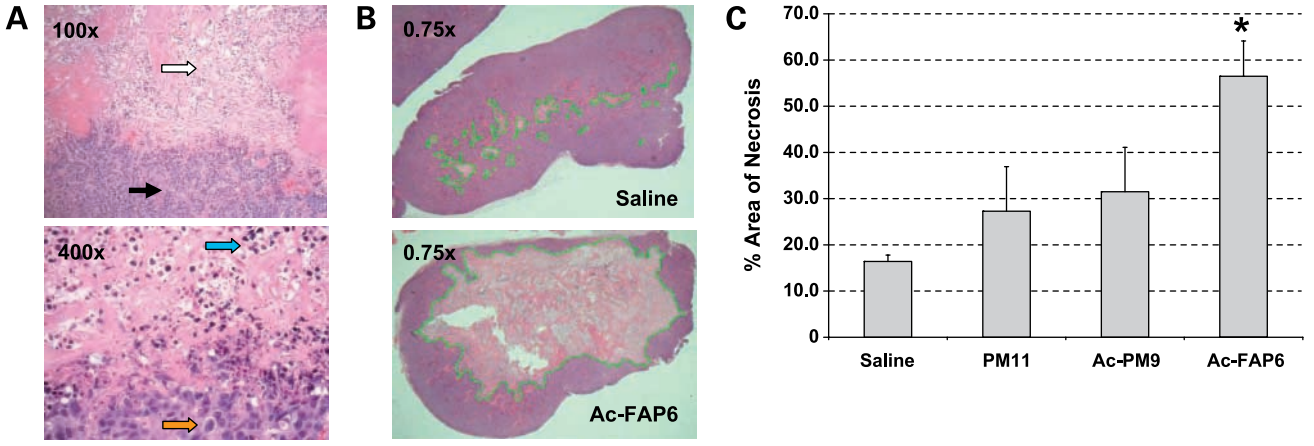

Figure 3. Comparison of the effect of promelittin toxins on the viability of human MCF-7 breast cancer xenografts. **A,** H&E-stained tissue from xenograft treated with Ac-FAP6 shows unaffected tumor adjacent to the necrotic area at ×100 and ×400 magnification. *Top, white arrow,* area of necrotic tissue; *black arrow,* strand of stroma within the background of tumor cells. *Bottom, blue arrow,* pyknotic nuclei consistent with necrotic death; *orange arrow,* nuclei from a viable cell unaffected by toxin; **B,** evaluation of the extent of necrosis produced by the intratumoral injection of Ac-FAP6 at 96 h postinjection. H&E-stained cross-section of representative tumor treated with either Ac-FAP6 (45 mg/kg) or saline shows increased areas of necrosis (*pale pink area outlined in green*) in a background of viable tumor (*reddish purple*). Representative images shown at ×0.75 magnification; **C,** image analysis used to the determine the % area of necrosis calculated as the ratio of the cross-sectional area of nonviable tumor to area of total tumor for tumors treated intratumorally with single dose of 250 nmoles of indicated toxin or normal saline (*, $P < 0.05$ by Student's t test for Ac-FAP6 versus saline control).

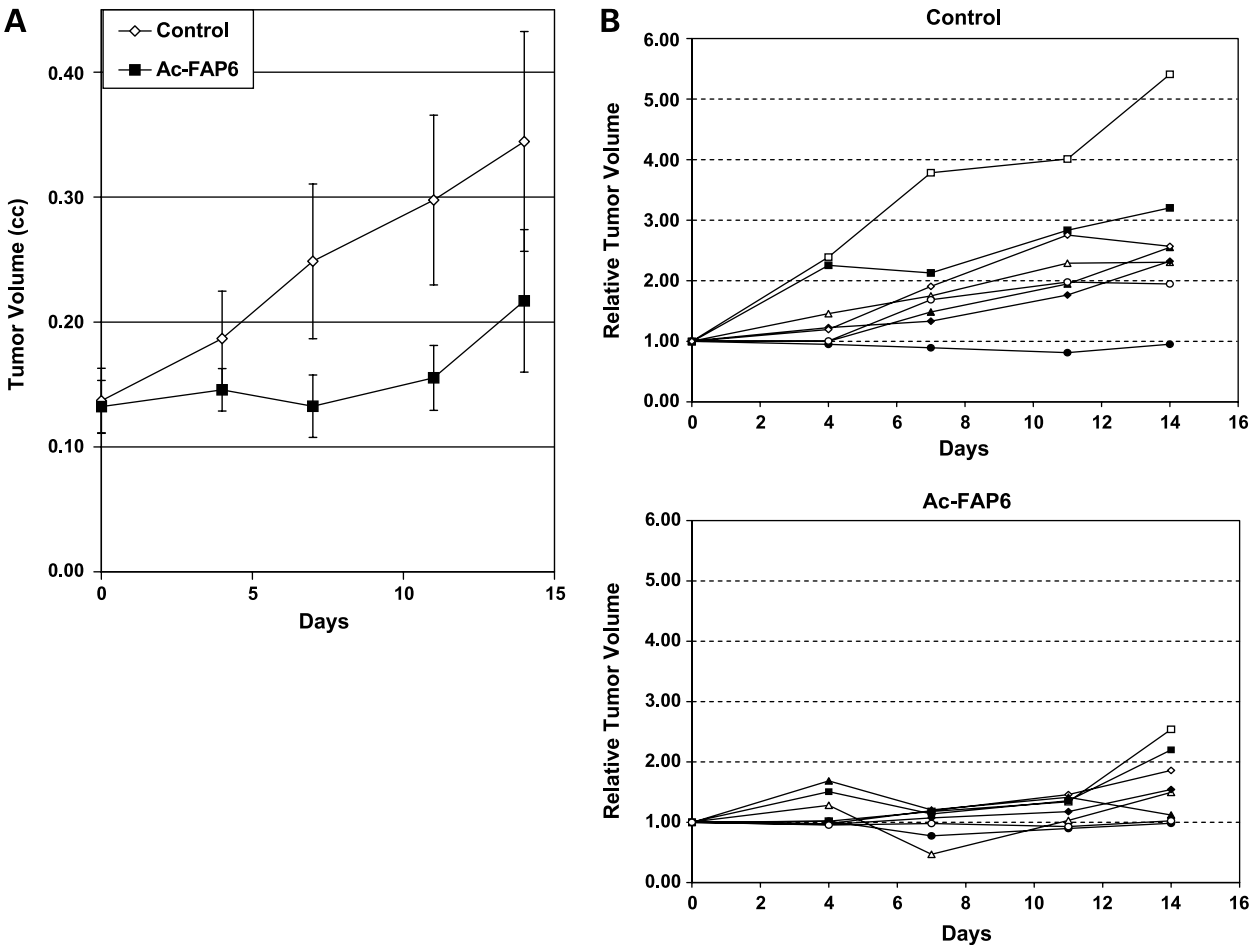

Figure 4. Antitumor effect of a single intratumoral dose of Ac-FAP6 against MCF-7 human breast cancer xenografts. **A,** average tumor volume of saline control versus Ac-FAP6 (45 mg/kg) over a 14-d period ($n = 8$ mice per group; $P < 0.05$ for days 4, 7, and 11 by ANOVA); **B,** growth of individual saline-treated control tumors to Ac-FAP6–treated tumors over a 14-d period. Each trace represents the growth of an individual MCF-7 xenograft in each mouse.

where intratumoral/intraorgan injection is possible. As an example of the applicability of such an approach, we described the development of a prostate-specific antigen–activated bacterial protoxin that is currently undergoing clinical testing as an intraprostatic therapy for the treatment of locally recurrent prostate cancer and benign prostatic hyperplasia (23). A similar strategy could be envisioned for the FAP-activated toxin. Because increased FAP expression has been found in most tumors evaluated, this approach could have a wider intratumoral application than that for a tissue-restricted protease such as prostate-specific antigen.

For these studies, we used an intratumoral treatment based approach to document that FAP-activated peptide toxin could produce a significant antitumor effect. Ideally, systemic delivery of these peptide toxins would be the preferred route administration. However, the ability of these promelittin toxins to induce hemolysis even when not fully processed represents a major hurdle to this application. In our hands, a single dose of 40 mg/kg of the FAP2 toxin, which was well-tolerated and effective intratumorally, proved lethal to tumor-bearing animals when administered i.v. This is most likely due to the fact that this dose would produce a potential maximum blood concentration that is >100 μmol/L, which is above the HD_{50} for this promelittin toxin. Further development of this promelittin peptide–based approach as a systemic therapy would require substantial modification to generate a protoxin that was unable to cause hemolysis even at millimolar concentrations. Alternatively, potent cytotoxic agents, preferably ones that did not produce hemolysis could be coupled to an FAP-specific peptide to generate an inactive prodrug that is selectively activated by FAP-expressing cells within the tumor stroma. Our laboratory has already adopted such an approach to generate prostate tissue specific prodrugs that are activated by the proteolytic activity of prostate-specific antigen, human glandular kallikrein 2, and prostate-specific membrane antigen (35–37). In ongoing studies in our laboratory, we are evaluating a series of such FAP-activated prodrugs that can be used to selectively target and kill cells within the tumor stroma as therapy for a wide variety of human cancers.

Disclosure of Potential Conflicts of Interest

No potential conflicts of interest were disclosed.

Acknowledgments

We thank Marc Rosen for the excellent technical assistance in performing animal studies and the Johns Hopkins School of Medicine Mass Spectrometry and Proteomics Core Facility for assistance with the characterization of peptide toxins.

References

1. Dvorak HF. Tumors: wounds that do not heal. Similarities between tumor stroma generation and wound healing. N Engl J Med 1986;315:1650–9.

2. Liotta LA, Steeg PS, Stetler-Stevenson WG. Cancer metastasis and angiogenesis: an imbalance of positive and negative regulation. Cell 1991;64:327–36.

3. Basset P, Bellocq JP, Wolf C, et al. A novel metalloproteinase gene specifically expressed in stromal cells of breast carcinomas. Nature 1990;348:699–704.

4. Brown LF, Guidi AJ, Schnitt SJ, et al. Vascular stroma formation in carcinoma *in situ*, invasive carcinoma, and metastatic carcinoma of the breast. Clin Cancer Res 1999;5:1041–56.

5. Haslam SZ, Woodward TL. Host microenvironment in breast cancer development: epithelial-cell-stromal-cell interactions and steroid hormone action in normal and cancerous mammary gland. Breast Cancer Res 2003;5:208–15.

6. Iozzo RV. Tumor stroma as a regulator of neoplastic behavior. Agonistic and antagonistic elements embedded in the same connective tissue. Lab Invest 1995;73:157–60.

7. Garin-Chesa P, Old LJ, Rettig WJ. Cell surface glycoprotein of reactive stromal fibroblasts as a potential antibody target in human epithelial cancers. Proc Natl Acad Sci U S A 1990;87:7235–9.

8. Aoyama A, Chen WT. A 170-kDa membrane-bound protease is associated with the expression of invasiveness by human malignant melanoma cells. Proc Natl Acad Sci U S A 1990;87:8296–300.

9. Piñeiro-Sánchez ML, Goldstein LA, Dodt J, et al. Identification of the 170-kDa melanoma membrane-bound gelatinase (seprase) as a serine integral membrane protease. J Biol Chem 1997;272:7595–601.

10. Scanlan MJ, Raj BK, Calvo B, et al. Molecular cloning of fibroblast activation protein α, a member of the serine protease family selectively expressed in stromal fibroblasts of epithelial cancers. Proc Natl Acad Sci U S A 1994;91:5657–61.

11. Rettig WJ, Garin-Chesa P, Beresford HR, Oettgen HF, Melamed MR, Old LJ. Cell-surface glycoproteins of human sarcomas: differential expression in normal and malignant tissues and cultured cells. Proc Natl Acad Sci U S A 1988;85:3110–4.

12. Tuxhorn JA, Ayala GE, Smith MJ, Smith VC, Dang TD, Rowley DR. Reactive stroma in human prostate cancer: induction of myofibroblast phenotype and extracellular matrix remodeling. Clin Cancer Res 2002;8:2912–23.

13. Cheng JD, Dunbrack RL, Jr., Valianou M, Rogatko A, Alpaugh RK, Weiner LM. Promotion of tumor growth by murine fibroblast activation protein, a serine protease, in an animal model. Cancer Res 2002;62:4767–72.

14. Ghilardi C, Chiorino G, Dossi R, Nagy Z, Giavazzi R, Bani M. Identification of novel vascular markers through gene expression profiling of tumor-derived endothelium. BMC Genomics 2008;9:201.

15. Kelly T. Fibroblast activation protein-α and dipeptidyl peptidase IV (CD26): cell-surface proteases that activate cell signaling and are potential targets for cancer therapy. Drug Resist Update 2005;8:51–8.

16. Park JE, Lenter MC, Zimmermann RN, Garin-Chesa P, Old LJ, Rettig WJ. Fibroblast activation protein, a dual specificity serine protease expressed in reactive human tumor stromal fibroblasts. J Biol Chem 1999;274:36505–12.

17. Aggarwal S, Brennen WN, Kole TP, et al. Fibroblast activation protein peptide substrates identified from human collagen I derived gelatin cleavage sites. Biochemistry 2008;47:1076–86.

18. Terwilliger TC, Eisenberg D. The structure of melittin. J Biol Chem 1982;257:6016–22.

19. Unger T, Oren Z, Shai Y. The effect of cyclization on magainin 2 and melittin analogues on the structure, function, and model membranes interactions: implications to their mode of action. Biochemistry 2001;40:6388–97.

20. Werkmeister JA, Hewish DR, Kirkpatrick A, Rivett DE. Sequence requirements for the activity of membrane active peptides. J Peptide Res 2002;60:232–8.

21. Hristova K, Dempsey CE, White SH. Structure, location and lipid perturbations of melittin at the membrane interface. Biophysical J 2001;80:801–11.

22. Kreil G, Haiml L, Suchanek G. Stepwise cleavage of the pro part of promelittin by dipeptidylpeptidase 4. Eur J Biochem 1980;111:49–58.

23. Williams SA, Merchant RF, Garrett-Mayer E, Isaacs JT, Buckley JT, Denmeade SR. A prostate-specific antigen-activated channel-forming toxin as therapy for prostatic disease. J Natl Cancer Inst 2007;99:376–85.

24. Aggarwal S, Singh P, Topaloglu O, Isaacs JT, Denmeade SR. A dimeric peptide that binds selectively to prostate-specific membrane antigen and inhibits its enzymatic activity. Cancer Res 2006;66:9171–7.

25. Edosada CY, Quan C, Wiesmann C, et al. Selective inhibition of fibroblast activation protein protease based on dipeptide substrate specificity. J Biol Chem 2006;281:7437–44.

26. Ostermann E, Garin-Chesa P, Heider KH, et al. Effective immunoconjugate therapy in cancer models targeting a serine protease of tumor fibroblasts. Clin Cancer Res 2008;14:4584–92.

27. Verel I, Heider KH, Siegmund M, et al. Tumor targeting properties of monoclonal antibodies with different affinity for target antigen CD44V6 in nude mice bearing head-and-neck cancer xenografts. Int J Cancer 2002;99:396–402.

28. Tahtis K, Lee FT, Wheatley JM, et al. Expression and targeting of human fibroblast activation protein in a human skin/severe combined immunodeficient mouse breast cancer xenograft model. Mol Cancer Ther 2003;2:729–37.

29. Scott AM, Wiseman G, Welt S, et al. A Phase I dose-escalation study of sibrotuzumab in patients with advanced or metastatic fibroblast activation protein-positive cancer. Clin Cancer Res 2003;9:1639–47.

30. Hofheinz RD, al-Batran SE, Hartmann F, et al. Stromal antigen targeting by a humanised monoclonal antibody: an early phase II trial of sibrotuzumab in patients with metastatic colorectal cancer. Onkologie 2003;26:44–8.

31. Adams S, Miller GT, Jesson MI, Watanabe T, Jones B, Wallner BP. PT-100, a small molecule dipeptidyl peptidase inhibitor, has potent antitumor effects and augments antibody-mediated cytotoxicity via a novel immune mechanism. Cancer Res 2004;64:5471–80.

32. Aertgeerts K, Levin I, Shi L, et al. Structural and kinetic analysis of the substrate specificity of human fibroblast activation protein α. J Biol Chem 2005;280:19441–4.

33. Wolf BB, Quan C, Tran T, Wiesmann C, Sutherlin D. On the edge of validation - cancer protease fibroblast activation protein. Mini-reviews in Med Chem 2008;8:719–727.

34. Ariga N, Sato E, Ohuchi N, Nagura H, Ohtani H. Stromal expression of fibroblast activation protein/seprase, a cell membrane serine proteinase and gelatinase, is associated with longer survival in patients with invasive ductal carcinoma of breast. Int J Cancer 2001;95:67–72.

35. Denmeade SR, Jakobsen CM, Janssen S, et al. Prostate-specific antigen-activated thapsigargin prodrug as targeted therapy for prostate cancer. J Natl Cancer Inst 2003;95:990–1000.

36. Janssen S, Rosen DM, Ricklis RM, et al. Pharmacokinetics, biodistribution, and antitumor efficacy of a human glandular kallikrein 2 (hK2)-activated thapsigargin prodrug. Prostate 2006;66:358–68.

37. Mhaka A, Gady AM, Rosen DM, Lo KM, Gillies SD, Denmeade SR. Use of methotrexate-based peptide substrates to characterize the substrate specificity of prostate-specific membrane antigen (PSMA). Cancer Biol Ther 2004;3:551–8.

Technical Abstract:

Background: It has been well documented that the tumor is dependent upon the reactive stroma for survival and growth signals, as well as, the nutritional support necessary for the maintenance of the primary mass. Additionally, the ability of the stroma to not only contribute to, but potentially drive, the progression of cancerous cells into a highly aggressive and metastatic phenotype is a concept that has only recently begun to be appreciated. The stroma has been shown to undergo morphological alterations, recruit reactive fibroblasts, macrophages, and lymphocytes, increase secretion of growth factors, signaling molecules and proteases, induce new blood vessel formation, as well as, produce an altered extracellular matrix when associated with a transformed epithelium. Fibroblasts, in particular, have been shown to consistently undergo several changes in both morphology and expression profiles when present in the tumor microenvironment. One defining characteristic of these carcinoma-associated fibroblasts, or myofibroblasts, is the expression of fibroblast activation protein-alpha (FAP). FAP is a membrane-bound serine protease that has both dipeptidase, as well as, gelatinase and collagenase activity. FAP is not expressed in healthy adults, but has been shown to be selectively expressed on myofibroblasts in the stroma surrounding >90% of epithelial cancers examined, including 7/7 human prostate cancer specimens, with minimal to no expression in either cancerous epithelial or adjacent normal tissues. FAP has been implicated in tumor promotion through studies demonstrating increases in tumor incidence, growth, and microvessel density using in vivo models. In contrast, other studies have shown that expression of FAP decreased tumorigenicity in vivo suggesting that the physiologic response to FAP may be dependent upon the exact context of its expression.

Objective/Hypothesis: Our goal is to evaluate FAP expression patterns and enzymatic activity in both normal prostate tissue and at various stages of oncogenic transformation (i.e. PIA, PIN, Localized and Advanced Cancer) to determine tumor stage in which FAP expression may play a role. A second objective is to exploit this expression in the treatment of prostate cancer by developing therapies targeted for activation by FAP. This will be accomplished by identifying selective peptide substrates for the proteolytic activity of FAP and coupling these peptides to a highly cytotoxic agent, thapsigargin, to generate prodrugs that are only activated in prostate tumors where FAP is expressed.

Specific Aims:

1) Characterize the expression patterns of FAP in normal prostate tissue and in the disease state.
2) Identify a FAP-specific cleavable peptide sequence for the development of targeted prodrugs.
3) Synthesize prodrug and measure kinetics in vitro.
4) Determine the potential therapeutic benefit and toxicity of this prodrug in vivo.

Study Design: We will generate and characterize clones of various prostate cancer cell lines (LNCaP, C4-2, C4-2B4, and PC3) expressing FAP or an empty vector control. Primary human prostate cancer tissue specimens representing varying stages of prostate cancer, as well as, adjacent normal tissue will be stained for FAP expression and quantified. FAP-specific peptide substrates will be identified in a complementary approach using a solution-phase phage display library and a positional scanning synthetic combinatorial library. Optimal substrate sequences will be coupled to thapsigargin, a highly cytotoxic compound. Kinetics of hydrolysis, as well as, specificity and stability will be measured in vitro using the FAP-expressing clones. Lead prodrugs identified in vitro will be used to treat xenografts derived from FAP-expressing clones and mock-transfected controls to determine potential therapeutic efficacy in vivo.

Impact: Metastatic epithelial cancers, such as those of the prostate, are composed of heterogeneous populations of cells that can have variable responses to anti-tumor agents. Currently utilized standard antiproliferative chemotherapies can produce modest improvement in survival in select cancer types, but are largely ineffective in treating malignancies of the prostate (proliferative index < 5%). Novel therapies that act in a proliferation-independent manner, therefore, are urgently needed for the treatment of advanced prostate cancer. An emerging strategy has been to target the stromal components associated with the tumor. One potential therapy is the development of prodrugs activated by proteases selectively expressed in the stromal compartment as outlined in this proposal. This approach will effectively deliver a cytotoxic molecule, such as thapsigargin, in a highly specific manner to the tumor microenvironment and will directly result in significant stromal cell death and indirectly in epithelial mortality due to a bystander effect with limited systemic toxicity.